DELIMITATING CRYPTIC SPECIES IN THE *GRACILARIA DOMINGENSIS* COMPLEX (GRACILARIACEAE, RHODOPHYTA) USING MOLECULAR AND MORPHOLOGICAL DATA[1]

Goia de M. Lyra[2]

Department of Organismic and Evolutionary Biology, Harvard University Herbaria, 22 Divinity Avenue, Cambridge Massachusetts 02138, USA

Programa de Pós-Graduação em Botânica, Universidade Estadual de Feira de Santana, Av. Transnordestina, s/n, Feira de Santana Bahia 44031-460, Brazil

Carlos Frederico D. Gurgel

The Environment Institute, Australian Centre for Evolutionary Biology and Biodiversity, School of Earth and Environmental Sciences, University of Adelaide, DX 650-418, Adelaide South Australia 5005, Australia

Department of Environment, Water and Natural Resources, State Herbarium of South Austrália, PO Box 2732, Kent Town South Australia 5071, Austrália

Departamento de Botânica, CCB, Universidade Federal de Santa Catarina, Florianópolis Santa Catarina 88040-900, Brazil

Instituto de Biociências, Universidade de São Paulo, Rua do Matão 277, São Paulo São Paulo 05508-090, Brazil

Emmanuelle da S. Costa

Instituto de Biociências, Universidade de São Paulo, Rua do Matão 277, São Paulo São Paulo 05508-090, Brazil

Priscila B. de Jesus

Programa de Pós-Graduação em Botânica, Universidade Estadual de Feira de Santana, Av. Transnordestina, s/n, Feira de Santana Bahia 44031-460, Brazil

Mariana C. Oliveira, Eurico C. Oliveira

Instituto de Biociências, Universidade de São Paulo, Rua do Matão 277, São Paulo São Paulo 05508-090, Brazil

Charles C. Davis

Department of Organismic and Evolutionary Biology, Harvard University Herbaria, 22 Divinity Avenue, Cambridge Massachusetts 02138, USA

and José Marcos de Castro Nunes

Laboratório de Algas Marinhas, Instituto de Biologia, Universidade Federal da Bahia, Rua Barão de Jeremoabo, s/n, Salvador Bahia 40170-115, Brazil

Species in the genus *Gracilaria* that display conspicuously flattened vegetative morphologies are a taxonomically challenging group of marine benthic red algae. This is a result of their species richness, morphological similarity, and broad phenotypic plasticity. Within this group, the *Gracilaria domingensis* complex is one of the most common, conspicuous, and morphologically variable species along the tropical western Atlantic Ocean. Previous research has identified that members of this complex belong to two distantly related clades. However, despite this increased phylogentic resolution, species delimitations within each of these clades remain unclear. Our study assessed the species diversity within this difficult complex using morphological and molecular data from three genetic markers (*cox*1, UPA, and *rbc*L). We additionally applied six single-marker species delimitation methods (SDM: ABGD, GMYCs, GMYCm, SPN, bPTP, and PTP) to *rbc*L, which were largely in agreement regarding species delimitation. These results, combined with our analysis of morphology, indicate that the *G. domingensis* complex includes seven distinct species, each of which are not all most closely related: *G. cervicornis*; a ressurected *G. ferox*; *G. apiculata* subsp. *apiculata*; a new species, *Gracilaria baiana* sp. nov.; *G. intermedia* subsp. *intermedia*; *G. venezuelensis*; and *G. domingensis* sensu stricto, which includes the later heterotypic synonym,

G. yoneshigueana. **Our study demonstrates the value of multipronged strategies, including the use of both molecular and morphological approaches, to decipher cryptic species of red algae.**

The marine red algal genus *Gracilaria* Greville is the largest genus in the order Gracilariales, and includes more than 200 species and 328 specific and infraspecific names (Guiry and Guiry 2016). *Gracilaria* species represent common and conspicuous members of marine benthic communities when they are present. Members of the genus are distributed in all tropical and temperate regions of the world, but the majority of its species are concentrated in the tropics. They are also economically important: they represent the main source of commercial agarose and numerous species produce secondary metabolites with potential antiviral, antibacterial, and antifungal properties (Almeida et al. 2011).

Gracilaria species exhibit a diverse range of growth forms, from completely cylindrical to flattened, ribbon-like thalli that can be simple or highly branched. Despite their simple gross morphology, the habits of many species display a wide range of overlapping phenotypes, often posing challenges for identification. This is especially problematic among species with flattened thalli, which were most recently circumscribed in Gracilariaceae (Gurgel and Fredericq 2004).

Among species with flattened thalli in *Gracilaria*, *G. domingensis* (Kützing) Sonder ex Dickie represents a species complex whose morphological diversity has intrigued taxonomists for decades. *Gracilaria domingensis* is a conspicuous species initially described from the Dominican Republic, with thalli that can grow to 40 cm in length and whose geographic distribution extends from the southern United States (Florida) to southern Brazil (Santa Catarina State; Oliveira et al. 1983, Gurgel and Fredericq 2004). Identification problems involving the circumscription of *G. domingensis* and morphologically similar species, including *G. cervicornis* (Turner) J.Agardh and *G. ferox* J.Agardh, have been noted since the 1980s (Oliveira et al. 1983). The habit of these three species exhibits a wide range of phenotypes within and between species. Moreover, small specimens can only be distinguished by either the examination of mature spermatangial conceptacles, which are not always present, or by molecular characters (Costa et al. 2012, Lyra et al. 2015).

Regarding the more recent taxonomy of the group, Oliveira et al. (1983) synonymized *G. ferox* with *G. cervicornis* on account of their overlapping morphologies. In this scheme, *G. cervicornis* has been distinguised from *G. domingensis* based on sexual features. Male reproductive structures in *G. domingensis* are characterized by deep spermatangial conceptacles (henriquesiana type, sensu Yamamoto 1984), while *G. cervicornis* are characterized by shallow cup-like conceptacles (textorii type, Oliveira et al. 1983). Spermatangial conceptacle type, whether forming shallow, cup-like pits (textorii type), horseshoe pits (verrucosa type), or deep confluent cavities in the thallus (henriquesiana type) have long been considered stable taxonomic characters for delimiting taxa in the Gracilariales (Gurgel and Fredericq 2004). However, applying phylogenetic analyses using DNA sequence data, Gurgel and Fredericq (2004) identified an unexpected placement of *G. domingensis* as immediately sister to *G. cervicornis*. This was unusual because *G. domingensis* was placed in a larger lineage characterized by taxa bearing only textorii-type spermatangia. Recent phylogentic investigations by Lyra et al. (2015), which greatly expanded the sampling of Gracilariaceae, and applied DNA barcoding and morphological approaches, however, have demonstrated that their accession of *G. domingensis* was misidentified, and was instead a species of *G. cervicornis*. This study further demonstrated that members of the *G. domingensis* complex were not monophyletic, and instead formed two distantly related clades. One well-supported clade included *G. domingensis* sensu stricto (s.s.), plus *G. yoneshigueana* Gurgel, Fredericq & J. Norris), *G. intermedia* J.Agardh subsp. *intermedia*, *G. venezuelensis* W.R.Taylor, and a fourth, potentially undescribed species. A second well-supported clade included *G. cervicornis*, *G. ferox*, and *G. apiculata* subsp. *apiculata* P.Crouan & H.Crouan. Within this second clade, *G. cervicornis* was well supported as nonmonophyletic. The combination of nonmonophyly of *G. cervicornis* plus a likely undescribed species closely related to *G. domingensis* s.s. indicated that this complex may harbor cryptic species, and thus be more complicated than previously thought (Lyra et al. 2015).

To better resolve the long-standing taxonomic uncertainties within the *G. domingensis* species complex, previous phylogenetic results need to be more fully explored using expanded molecular sampling and a thoughtful investigation of morphology. Here, we present a three-pronged approach to achieve our goal: multimarker phylogenetic analysis, species delineation methods (SDMs), and morphological assessments.

MATERIALS AND METHODS

We analyzed a total of 140 specimens from across the range of the *G. domingensis* complex (Table 1). The majority

of these specimens were collected during the last 20 years, largely by coauthors of our paper. However, only the more recent samples were preserved in a manner that renders them amenable for downstream genetic analyses (i.e., dried in silica gel). All specimens were investigated for morphology, but we sampled only 24 of these specimens successfully for DNA analysis (some of which were previously published by Lyra et al. 2015 and Gurgel and Fredericq 2004; Table 1). Our molecular sampling focused especially on the two subclades identified by Lyra et al. (2015) that constitute the *G. domingensis* complex. Of the seven potential species assigned to these two clades, we sampled four of them extensively. These included *G. domingensis*, *G. cervicornis*, *G. ferox*, and a fourth, potentially undescribed species. Our rational for deeper sampling of these species is that their morphology is largely similar, thus making circumscription more challenging. Moreover, as we indicated in the Introduction, we wanted to further explore the limits of a potentially undescribed species and better characterize *G. cervicornis*, which was identified as nonmonophyletic. The remaining three species—*G. intermedia* subsp. *intermedia*, *G. venezuelensis*, and *G. apiculata* subsp. *apiculata*—are very well characterized (Gurgel et al. 2004a,b), and thus less well sampled here. The biogeographic sampling of specimens for our analyses ranged from tropical to subtropical areas, from southern Brazil to Florida, United States, including type specimens.

Molecular analyses. We generated DNA sequences for three markers, cytochrome oxidase I (*cox*1), the Universal Plastid Amplicon (UPA), and the large subunit of the ribulose 1–5 biphosphate carboxilase oxigenase (*rbc*L). Total DNA was extracted from ~20 to 40 mg of samples by maceration in liquid nitrogen using the procedure outlined by Faugeron et al. (2001), or alternatively using the Chelex method described by Cohen et al. (2004). Molecular markers were PCR amplified under the following conditions: 1× PCR buffer, 1.5 mM MgCl$_2$, 0.2 mM each dNTP, 0.2 μM of each primer, 5 ng of genomic DNA, and 1.25 U of Taq DNA polymerase (Invitrogen, Carlsbad, CA, USA, or Qiagen, Valencia, CA, USA) for a total volume of 25 μL. The amplification and sequencing reaction for *cox*1 used the primers GazF1 and GazR1 (Saunders 2005); *rbc*L used primers FrbcL and RrbcS (Freshwater and Rueness 1994) plus the additional internal primers R753 and F492 (Freshwater and Rueness 1994); and UPA used primers p23Sv_f1 and p23Sv_r1 (Sherwood and Presting 2007). PCR was performed with an initial denaturation step at 94°C for 10 min, followed by 35 cycles of 30 s at 90°C, 30 s at 50°C (variations of 47°C and 55°C for *rbc*L and UPA, respectively), and 2 min at 72°C, with a final 10 min extension cycle at 72°C. PCR products were sequenced in both directions using dye terminators and sequencing protocols at GeneWiz (Cambridge, MA, USA, http://www.genewiz.com/). Sequences were deposited in the Barcode of Life Data Systems (http://www.boldsystems.org/) and GenBank (Table 1).

Phylogenetic analyses. Chromatograms were assembled and edited using Geneious v6.0.6 (Drummond et al. 2011). Phylogenetic relationships were estimated using maximum likelihood (ML) and Bayesian methods. Our ML analyses were conducted using RAxML v7.2.8 (Stamatakis 2006) with a single GTRGAMMA model. The best-scoring ML tree and 200 bootstrap trees were obtained using the rapid hill-climbing algorithm (Stamatakis et al. 2008). The Bayesian analyses were implemented using the parallel version of BayesPhylogenies v2.0 (Pagel and Meade 2004) with a reversible-jump implementation of the mixture model as described by Venditti et al. (2008). This approach allows the fitting of multiple models of sequence evolution to each character in an alignment without a priori partitioning, and has been previously implemented successfully for large-scale phylogenetic analyses (Xi et al. 2012). Two independent Markov chain Monte Carlo

(MCMC) analyses were performed, and the consistency of stationary-phase likelihood values and estimated parameter values was determined using Tracer v1.5. We ran each MCMC analysis for 10 million generations, with trees and parameters sampled every 1,000 generations. Bayesian posterior probabilities (PP; converted to percentages throughout) were determined by building a 50% majority-rule consensus tree from two MCMC analyses after discarding the initial 20% burn-in generations. Other genera of Gracilariaceae were used as outgroups following Lyra et al. (2015). We analyzed each marker individually, but did not concatenate these data due to the lack of overlapping sequences for *rbc*L, *cox*1, and UPA.

UPA and *cox*1 were shorter (300 and 597 bp for UPA and *cox*1, respectively; versus 1,071 for *rbc*L) and less informative (0.14% and 0.33% parsimony informative characters per site for UPA and *cox*1, respectively; versus 0.37% for *rbc*L). Additionally, owing to the availability of data in GenBank, *rbc*L was much better sampled across our ingroup. Taking these three factors into account—marker length, informativeness, and taxon sampling—we applied six SDMs only to the *rbc*L data set. The automated barcode gap discovery (ABGD) method of Puillandre et al. (2012a), calculates a single, model-based, one-sided confidence limit for intraspecific divergences observed across the entire DNA alignment. A threshold level of genetic diversity is determined from the first significant gap beyond this limit, and is used to partition the data into phylogenetic species hypotheses. We used the statistical parsimony network (SPN) reconstruction method implemented in TCS v.1.21 (Clement et al. 2000) with a confidence limit of 99% to identify clusters of closely related sequences corresponding to distinct species. Using SPN, different genetic species emerge as unconnected sequences or networks due to their greater evolutionary distinctness as measured by mutations. The General Mixed Yule Coalescent (GMYC) model can be run using single (GMYC$_S$) and mutiple (GMYC$_M$) delimiting thresholds under a ML framework (Pons et al. 2006; Monaghan et al. 2009). GMYC techniques use an ultrametric phylogeny to determine the transition signal from intraspecific lineage branching patterns (i.e., a coalescent model, Wakeley 2009) to interspecific or speciation branching patterns (i.e., a Yule stochastic model, Yule 1925). The point of transition is determined as the threshold point beyond which clades are considered distinct species. Lastly, we also assessed species delimitation via the recently developed Poisson Tree Process (PTP) model of Zhang et al. (2013), which includes a ML (PTP) and a Bayesian implementation (bPTP). Here, we applied a threshold of 75% bootstrap support to define species. This threshold is higher than the widely used 70% bootstrap percentage cut-off often associated with 95% confidence that the clade is likely real (Hillis and Bull 1993).

For each of the six SDMs (ABGD, SPN, GMYCs, GMYCm, PTP, bPTP) the input files and parameters are summarized as follows. For ABGD, a FASTA alignment was used in the online implementation (http://wwwabi.snv.jussieu.fr/public/abgd/abgdweb.html) using optimum parameter settings as follows: pmin = 0.001, pmax = 0.10, a relative width gap (*x*-value) of 1.1, minimum slope = 0.001, number of bins = 20, and JC69 (Jukes-Cantor 1969). For GMYC, an ultrametric tree was generated in BEAST, estimated with a lognormal relaxed clock (uncorrelated), with a rate of 1.0, using a calibrated Yule Tree Prior. After confirming that the topology of the ultrametric tree was the same as those obtained via ML and Bayesian methods, this Newick-formatted tree was used as the input file in the online versions of the single and multiple threshold implementations of the GMYC (http://species.h-its.org/gmyc/). For PTP and bPTP, the Newick-formatted ML tree described above was used as the input file in the online implementation of PTP/bPTP (http://species.h-its.org/ptp/). Here, we applied

TABLE 1. Voucher information with herbarium and GenBank accession information. Herbarium acronyms follow *Index Herbariorum* (Holmgren et al. 1990). NA, voucher number not available; –, no molecular data were produced; newly generated sequences presented in bold face.

Taxon	Voucher	Locality	cox1	UPA	rbcL
					Genbank accession numbers
Gracilaria apiculata P.Crouan & H.Crouan	C.F. Gurgel s.n. (LAF, NA)	Venezuela, Falcón State, Peninsula Paraguana, La Encrujijada	–	–	AY049333
	Collector unknown (lectotype; BM00936189)	French West Indies, Guadeloupe, Marie–Galante, Grand–Bourg	–	–	–
Gracilaria baiana sp. nov.	G.M. Lyra and J.M.C. Nunes (holotype; ALCB103804)	Brazil, Bahia, Vera Cruz, Penha	–	**KT353014**	KP210241
	G.M. Lyra and J.M.C. Nunes (isotype; ALCB103799)	Brazil, Bahia, Vera Cruz, Penha	KP210196	KP403234	KP210243
	G.M. Lyra and J.M.C. Nunes (paratype; ALCB103788)	Brazil, Bahia, Vera Cruz, Penha	**KT353012**	–	–
	G.M. Lyra and J.M.C. Nunes (paratype; ALCB103789)	Brazil, Bahia, Vera Cruz, Penha	–	**KP403233**	KP210242
	G.M. Lyra and J.M.C. Nunes (paratype; ALCB103245)	Brazil, Bahia, Vera Cruz, Penha	–	–	–
	G.M. Lyra and J.M.C. Nunes (paratype; ALCB103246)	Brazil, Bahia, Vera Cruz, Penha	–	–	–
	C.F.D. Gurgel (paratype; LAF NA)	Brazil, Bahia, Vera Cruz, Penha	–	–	–
Gracilaria cervicornis (Turner) J. Agardh	G. M. Lyra (ALCB65155)	Brazil, Bahia, Ilhéus, Gravatá	–	KP403181	–
	J.M.C. Nunes and A.M Netto (ALCB57507)	Brazil, Bahia, Ilhéus, Gravatá	–	–	–
	J.M.C. Nunes et al. (ALCB57514)	Brazil, Bahia, Ilhéus, Gravatá	–	–	–
	G.M. Lyra and J.M.C. Nunes (ALCB103172)	Brazil, Bahia, Santa Cruz de Cabrália, Apuã	–	–	**KT601638**
	G.M. Lyra and J.M.C. Nunes (ALCB103145)	Brazil, Bahia, Entre Rios, Subaúma	**KT353011**	–	–
	G.M. Lyra and J.M.C. Nunes (ALCB103175)	Brazil, Bahia, Entre Rios, Subaúma	KP210156	–	KP210219
	A.M. Lucio (ALCB34737)	Brazil, Bahia, Camaçari, Guarajuba	–	–	–
	A.M. Netto (ALCB22306)	Brazil, Bahia, Olivença	–	–	–
	J.M.C. Nunes and A.M. Netto (ALCB57509)	Brazil, Bahia, Itacaré, Engenhoca	–	–	–
	J.M.C. Nunes and A.M. Netto (ALCB53540)	Brazil, Bahia, Itacaré, Engenhoca	–	–	–
	J.M.C. Nunes and A.M. Netto (ALCB61020)	Brazil, Bahia, Itacaré, Engenhoca	–	–	–
	J.M.C. Nunes and A.M. Netto (ALCB60855)	Brazil, Bahia, Itacaré, Engenhoca	–	–	–
	J.M.C. Nunes (ALCB57511)	Brazil, Bahia, Mata de São João, Praia do Forte	–	–	–
	J.M.C. Nunes and G.M. Lyra (ALCB57504)	Brazil, Bahia, Prado, Cumuruxatiba	–	–	–
	J.M.C. Nunes et al. (ALCB52952)	Brazil, Bahia, Porto Seguro, Mucugê	–	–	–
	J.M.C. Nunes et al. (ALCB49578)	Brazil, Bahia, Saubara, Recifes de Saubara	–	–	–
	J.M.C. Nunes (ALCB68516)	Brazil, Bahia, Vera Cruz, Penha	–	–	–
	E. Plastino (SPF56873)	Brazil, Rio Grande do Norte, Rio do Fogo	–	KP403177	–
	C.F. Gurgel (LAF, NA)	Brazil, Rio de Janeiro, Búzios, Praia Rasa	–	–	AY049371
	Dr. Wright (lectotype; BM00936191)	Jamaica	–	–	–
Gracilaria domingensis Sonder ex Kützing	G.M. Lyra (ALCB65141)	Brazil, Bahia, Uruçuca,Serra Grande	**KP210175**	**KP403207**	KP210223
	G.M. Lyra (ALCB60649)	Brazil, Bahia, Uruçuca,Serra Grande	**KT353009**	–	KP210222
	G.M. Lyra (ALCB99648)	Brazil, Bahia, Santa Cruz de Cabrália, Coroa Vermelha	–	–	**KP210226**
	J.M.C. Nunes (ALCB49531)	Brazil, Bahia, Jauá	–	–	–
	J.M.C. Nunes (ALCB52787)	Brazil, Bahia, Conde, Barra do Itariri	–	–	–
	J.M.C. Nunes et al. (ALCB57550)	Brazil, Bahia, Esplanada, Baixio	–	–	–
	J.M.C. Nunes et al. (ALCB57551)	Brazil, Bahia, Esplanada, Baixio	–	–	–
	J.M.C. Nunes and A.M. Netto (ALCB57507)	Brazil, Bahia, Ilhéus, Gravatá	–	–	–

TABLE 1. (continued)

Taxon	Voucher	Locality	Genbank accession numbers		
			*cox*1	UPA	*rbcL*
	J.M.C. Nunes and A.M. Netto (ALCB57556)	Brazil, Bahia, Ilhéus, Gravatá	–	–	–
	J.M.C. Nunes and A.M. Netto (ALCB57560)	Brazil, Bahia, Ilhéus, Gravatá	–	–	–
	J.M.C. Nunes and A.M. Netto (ALCB57791)	Brazil, Bahia, Ilhéus, Gravatá	–	–	–
	J.M.C. Nunes and A.M. Netto (ALCB57792)	Brazil, Bahia, Ilhéus, Gravatá	–	–	–
	J.M.C. Nunes et al. (ALCB53173)	Brazil, Bahia, Ilhéus, Gravatá	–	–	–
	J.M.C. Nunes et al. (ALCB57557)	Brazil, Bahia, Ilhéus, Gravatá	–	–	–
	J.M.C. Nunes et al. (ALCB57558)	Brazil, Bahia, Ilhéus, Gravatá	–	–	–
	J.M.C. Nunes et al. (ALCB57559)	Brazil, Bahia, Ilhéus, Gravatá	–	–	–
	A.M. Netto (ALCB22334)	Brazil, Bahia, Ilhéus, Morro de Pernambuco	–	–	–
	A.M. Netto et al. (ALCB49393)	Brazil, Bahia, Ilhéus, Olivença	–	–	–
	J.M.C. Nunes and A.M. Netto (ALCB57506)	Brazil, Bahia, Itacaré, Engenhoca	–	–	–
	J.M.C. Nunes and A.M. Netto (ALCB57555)	Brazil, Bahia, Itacaré, Engenhoca	–	–	–
	J.M.C. Nunes and A.M. Netto (ALCB57748)	Brazil, Bahia, Itacaré, Engenhoca	–	–	–
	J.M.C. Nunes and A.M. Netto (ALCB60855)	Brazil, Bahia, Itacaré, Engenhoca	–	–	–
	J.M.C. Nunes and A.M. Netto (ALCB61027)	Brazil, Bahia, Itacaré, Engenhoca	–	–	–
	J.M.C. Nunes and G.M. Lyra (ALCB57502)	Brazil, Bahia, Prado, Cumuruxatiba	–	–	–
	J.M.C. Nunes and G.M. Lyra (ALCB57503)	Brazil, Bahia, Prado, Cumuruxatiba	–	–	–
	J.M.C. Nunes and G.M. Lyra (ALCB57504)	Brazil, Bahia, Prado, Cumuruxatiba	–	–	–
	J.M.C. Nunes and G.M. Lyra (ALCB57505)	Brazil, Bahia, Prado, Cumuruxatiba	–	–	–
	J.M.C. Nunes and G.M. Lyra (ALCB57545)	Brazil, Bahia, Prado, Cumuruxatiba	–	–	–
	J.M.C. Nunes and G.M. Lyra (ALCB57546)	Brazil, Bahia, Prado, Cumuruxatiba	–	–	–
	J.M.C. Nunes et al. (ALCB65152)	Brazil, Bahia, Salvador, Paramana	–	–	–
	J.M.C. Nunes (ALCB60798)	Brazil, Bahia, Lauro de Freitas, Ipitanga	–	–	–
	J.M.C. Nunes (ALCB60799)	Brazil, Bahia, Lauro de Freitas	–	–	–
	J.M.C. Nunes (ALCB60800)	Brazil, Bahia, Lauro de Freitas	–	–	–
	J.M.C. Nunes (ALCB60803)	Brazil, Bahia, Lauro de Freitas, Ipitanga	–	–	–
	J.M.C. Nunes et al. (ALCB49247)	Brazil, Bahia, Saubara, Recifes de Saubara	–	–	–
	J.M.C. Nunes et al. (ALCB49356)	Brazil, Bahia, Saubara, Recifes de Saubara	–	–	–
	J.M.C. Nunes et al. (ALCB60974)	Brazil, Bahia, Saubara, Recifes de Saubara	–	–	–
	J.M.C. Nunes et al. (ALCB61012)	Brazil, Bahia, Saubara, Recifes de Saubara	–	–	–
	J.M.C. Nunes and A.M. Netto (ALCB53242)	Brazil, Bahia, Diogo	–	–	–
	J.M.C. Nunes and A.M. Netto (ALCB53243)	Brazil, Bahia, Diogo	–	–	–
	J.M.C. Nunes (ALCB57508)	Brazil, Bahia, Vera Cruz, Barra Grande	–	–	–
	J.M.C. Nunes (ALCB57469)	Brazil, Bahia, Vera Cruz, Cacha–Prego	–	–	–
	A. Taouil (LAF, NA)	Brazil, Rio de Janeiro, Arraial do Cabo	–	–	AY049372
	Collector unknown (holotype; MEL44407)	Dominican Republic, Hispaniola, Santo Domingo Island	–	–	–

(continued)

TABLE 1. (continued)

Taxon	Voucher	Locality	Genbank accession numbers		
			*cox*I	UPA	*rbcL*
Gracilaria ferox J. Agardh	E. Oliveira (SPF56868)	Brazil, São Paulo, Ubatuba, Praia do Costa	**KT353010**	**KP403212**	–
	J.M.C. Nunes and G.M. Lyra (ALCB65143)	Brazil, Bahia, Porto Seguro, Mucugê	KP210155	KP403182	–
	J.M.C. Nunes and G.M. Lyra (ALCB52953)	Brazil, Bahia, Porto Seguro, Mucugê	–	–	–
	J.M.C. Nunes and G.M. Lyra (ALCB52954)	Brazil, Bahia, Porto Seguro, Mucugê	–	–	–
	J.M.C. Nunes and G.M. Lyra (ALCB53056)	Brazil, Bahia, Porto Seguro, Mucugê	–	–	–
	S.M.P.B. Guimarães (ALCB65154)	Brazil, Bahia, Porto Seguro, Mucugê	–	–	–
	A.M. Netto (ALCB48280)	Brazil, Bahia, Porto Seguro, Arraial D'Ajuda	–	–	–
	J.M.C. Nunes and G.M. Lyra (ALCB57497)	Brazil, Bahia, Porto Seguro, Arakakaí	–	–	–
	J.M.C. Nunes and G.M. Lyra (ALCB57788)	Brazil, Bahia, Porto Seguro, Arakakaí	–	–	–
	J.M.C. Nunes and G.M. Lyra (ALCB61060)	Brazil, Bahia, Porto Seguro, Arakakaí	–	–	–
	J.M.C. Nunes and G.M. Lyra (ALCB103169)	Brazil, Bahia, Santa Cruz de Cabrália, Apuã	**KT353013**	**KP403178**	–
	J.M.C. Nunes and A.M. Netto (ALCB53211)	Brazil, Bahia, Ilhéus, Gravatá	–	–	–
	J.M.C. Nunes and A.M. Netto (ALCB57510)	Brazil, Bahia, Ilhéus, Gravatá	–	–	–
	J.M.C. Nunes and A.M. Netto (ALCB60906)	Brazil, Bahia, Ilhéus, Gravatá	–	–	–
	J.M.C. Nunes and A.M. Netto (ALCB61031)	Brazil, Bahia, Ilhéus, Gravatá	–	–	–
	J.M.C. Nunes et al. (ALCB53406)	Brazil, Bahia, Ilhéus, Gravatá	–	–	–
	J.M.C. Nunes et al. (ALCB57515)	Brazil, Bahia, Ilhéus, Gravatá	–	–	–
	A.M. Netto (ALCB48461)	Brazil, Bahia, Ilhéus, Olivença	–	–	–
	J.M.C. Nunes and A.M. Netto (ALCB61021)	Brazil, Bahia, Itacaré, Engenhoca	–	–	–
	G.M. Lyra et al. (ALCB48346)	Brazil, Bahia, Itacaré, Praia da Concha	–	–	–
	A.M. Netto et al. (ALCB34815)	Brazil, Bahia, Uruçuca, Serra Grande	–	–	–
	A.M. Netto et al. (ALCB49127)	Brazil, Bahia, Uruçuca, Serra Grande	–	–	–
	M.E.C. Ramos (ALCB52438)	Brazil, Bahia, Cairú, Garapuá	–	–	–
	M.E.C. Ramos (ALCB53208)	Brazil, Bahia, Cairú, Garapuá	–	–	–
	M.E.C. Ramos (ALCB53427)	Brazil, Bahia, Cairú, Garapuá	–	–	–
	M.E.C. Ramos (ALCB53438)	Brazil, Bahia, Cairú, Garapuá	–	–	–
	J.M.C. Nunes and A.M. Netto (ALCB49430)	Brazil, Bahia, Cairú, Morro de São Paulo	–	–	–
	J.M.C. Nunes and A.M. Netto (ALCB52754)	Brazil, Bahia, Cairú, Morro de São Paulo	–	–	–
	J.M.C. Nunes (ALCB53387)	Brazil, Bahia, Salvador, Ilha de Maré, Tapera	–	–	–
	J.M.C. Nunes (ALCB49209)	Brazil, Bahia, Salvador, Stella Maris	–	–	–
	J.M.C. Nunes (ALCB57471)	Brazil, Bahia, Salvador, Stella Maris	–	–	–
	J.M.C. Nunes (ALCB57681)	Brazil, Bahia, Salvador, Stella Maris	–	–	–
	J.M.C. Nunes (ALCB60802)	Brazil, Bahia, Lauro de Freitas, Ipitanga	–	–	–
	Cepemar (ALCB22164)	Brazil, Bahia, Camaçari, Arembepe	–	–	–
	J.M.C. Nunes and A.M. Lucio (ALCB34736)	Brazil, Bahia, Mata de São João, Guarajuba	–	–	–
	J.M.C. Nunes and A.M. Lucio (ALCB49519)	Brazil, Bahia, Mata de São João, Guarajuba	–	–	–
	A.M. Lucio (ALCB34734)	Brazil, Bahia, Mata de São João, Guarajuba	–	–	–
	A.M. Lucio (ALCB34735)	Brazil, Bahia, Mata de São João, Guarajuba	–	–	–
			–	–	–

(continued)

TABLE 1. (continued)

Taxon	Voucher	Locality	cox1	UPA	rbcL
			Genbank accession numbers		
	J.M.C. Nunes and M. Altamirano (ALCB22213)	Brazil, Bahia, Mata de São João, Itacimirim			
	J.M.C. Nunes and M. Altamirano (ALCB49518)	Brazil, Bahia, Mata de São João, Itacimirim	–	–	–
	Y. Braga and F. Kelmo (ALCB60744)	Brazil, Bahia, Mata de São João, Itacimirim	–	–	–
	J.M.C. Nunes and M. Altamirano (ALCB22385)	Brazil, Bahia, Mata de São João, Praia do Forte	–	–	–
	J.M.C. Nunes (ALCB49515)	Brazil, Bahia, Mata de São João, Praia do Forte	–	–	–
	J.M.C. Nunes (ALCB52772)	Brazil, Bahia, Mata de São João, Praia do Forte	–	–	–
	J.M.C. Nunes (ALCB57512)	Brazil, Bahia, Mata de São João, Praia do Forte	–	–	–
	J.M.C. Nunes (ALCB57513)	Brazil, Bahia, Mata de São João, Praia do Forte	–	–	–
	J.M.C. Nunes et al. (ALCB49572)	Brazil, Bahia, Mata de São João, Saubara, Recifes de Saubara	–	–	–
	J.M.C. Nunes (ALCB49521)	Brazil, Bahia, Vila de Abrantes, Jauá	–	–	–
	J.M.C. Nunes et al. (ALCB65155)	Brazil, Bahia, Entre Rios, Subaúma	–	–	–
	J.M.C. Nunes (ALCB53542)	Brazil, Bahia, Vera Cruz, Cacha –Prego	–	–	–
	J.M.C. Nunes (ALCB57470)	Brazil, Bahia, Vera Cruz, Cacha –Prego	–	–	–
	J.M.C. Nunes (ALCB22390)	Brazil, Bahia, Vera Cruz, Penha	–	–	–
	J.M.C. Nunes (ALCB49520)	Brazil, Bahia, Vera Cruz, Penha	–	–	–
	C.F. Gurgel (LAF, NA)	United States, Florida, Higgis Beach, Key West	–	–	AY049365
	C.F. Gurgel (LAF, NA)	United States, Florida, Higgis Beach, Key West	–	–	AY049366
	C.F. Gurgel (LAF, NA)	United Sates, Florida, Higgis Beach, Key West	–	–	AY049367
	C.F. Gurgel (LAF, NA)	United States, Florida, Bahia Honda, Florida Keys	–	–	AY049368
	(lectotype; NY01089159)	Martinique	–	–	–
Gracilaria intermedia J.Agardh subsp. *intermedia*	C.F. Gurgel et al. (LAF, NA)	Venezuela, Falcón State, Peninsula Paraguana, Buchuaco	–	–	AY049335
	J. MacLachlan and T. Edelstein (FH, NA)	Canada, Nova Scotia, Pomquet Harbour	–	–	–
	G.A. Hall (lectotype; LD29649)	United States, Florida, St. Augustine	–	–	–
Gracilaria venezuelensis W.R.Taylor	C.F. Gurgel (LAF, NA)	United States, Florida, Fort Pierce	–	–	AF539603
	W.R. Taylor (holotype; MICH1306428)	Venezuela, Nueva Esparta, Station No. A27	–	–	–
G. yoneshigueana Gurgel, Fredericq & J. Norris	A. Taouil (holotype; US204329)	Brazil, Rio de Janeiro, Prainha	–	–	AY049372

100,000 MCMC generations with thinning to 100 and burn-in to 10% using a five-digit random seed generator.

Morphology. Living samples of the 140 specimens that we analyzed were collected in the field, transported to the laboratory, cleaned, and sorted carefully under a stereomicroscope (Leica® Zoom 2000, Leica Microsystems GmbH - Wetzlar, Germany). Materials for morphological investigation were preserved in 4% formalin in seawater. For each of the more recently collected samples, three to five pieces of thalli were preserved in silica gel for subsequent DNA extraction. Dried herbarium vouchers were deposited in the following herbaria: ALCB, SPF, LAF, and FH (herbarium abbreviations follow Thiers 2014). Additionally, the type specimens of *G. cervicornis* (BM000936191), *G. domingensis* (MEL44407), *G. apiculata* subsp. *apiculata* (BM00936189), *G. intermedia* subsp. *intermedia* (LD29649), *G. venezuelensis* (MICH1306428), and *G. yoneshigueana* Gurgel, Fredericq & J. Norris (US204329), plus images of *G. ferox* type material from Martinique (NYBG; NY01089159) were carefully analyzed. Manual cross-sections for morphological studies were conducted using stainless steel razor blades, and stained in a 3% aniline blue solution for 5 min (Tsuda and Abbott 1985). Photomicrographs were taken with a Q Imaging GO-3 digital camera (Olympus, Tokyo, Japan) attached to an Olympus CX31 microscope. Images were edited and assembled using Photoshop CS6 (Adobe Systems Inc., San Jose, CA, USA).

A comparison between our results from the six SDMs, three phylogenetic markers, and morphology was used to delimit species and to propose a revised taxonomy for the group. *G. apiculata* subsp. *apiculata*, *G. intermedia* subsp. *intermedia*, and *G. venezuelensis* are well characterized and have been illustrated elsewhere (Gurgel et al. 2004a,b). Below we provide descriptions and illustrations for the remaining four species. Lastly, we also include a dichotomous key for the identification of all seven members of the *G. domingensis* complex.

RESULTS

Phylogenetic analyses. A total of 25 sequences (from 15 specimens) were newly generated for our study (eight *cox*1, eight UPA, and nine *rbc*L sequences). These were added to 25, 28, and 86 published *cox*1, UPA, and *rbc*L sequences, respectively. The length of the alignments, the number of variable nucleotide positions, and the number of parsimonious informative sites for *cox*1, UPA, and *rbc*L were, respectively: 597 bp, 241, 195; 300 bp, 67, 43; and 1,071 bp, 454, 393. Tree topologies for all three markers were not in conflict above 75% bootstrap percentage (BP; Figs. 1–3). The *rbc*L topology was the most well-resolved (Fig. 3).

The ML and Bayesian topologies of all three markers identified seven distinct and largely well-supported subclades among members of the *G. domingensis* species complex. These clades correspond to our proposed species circumscriptions (Figs. 1–3). Moreover, we did not infer well-supported nested clades within each of these subclades. In combination with our SDMs and morphology (see below) we recognized each of these seven subclades as species: *G. cervicornis*, *G. ferox*, *G. apiculata* subsp. *apiculata* (clade I), *G. domingensis*, *G. intermedia* subsp. *intermedia*, *G. venezuelensis*, and *G. baiana* sp. nov. (clade II). *G. cervicornis* is supported by <50% BP, and <50% PP for *cox*1 and for UPA, and 100% BP and 100% PP for *rbc*L. *G. ferox* is supported by 99% BP and 100% PP for *cox*1; 100% BP and 86% PP for UPA, and 100% BP and 100% PP for *rbc*L. The *G. domingensis* [= *G. domingensis* s.s.] clade was supported by 100% BP and PP for *cox*1; 87% BP and <50% PP for UPA; 77% BP and 99% PP for *rbc*L. The new species, *G. baiana* sp. nov. is supported by 100% BP and 98% PP for *cox*1; 91% BP and 86% PP for UPA, 100% BP and PP for *rbc*L. *G. apiculata* subsp. *apiculata*, *G. intermedia* subsp. *intermedia*, and *G. venezuelensis* were only represented by single accessions in the *rbc*L phylogeny.

Finally, newly generated DNA sequences from recently collected specimens whose morphologies match the type of *G. domingensis* s.s. (ALCB65141, ALCB60649, ALCB99648; Table 1) also match GenBank accessions previously identified as *G. yoneshigueana* (100% *rbc*L sequence similarity). This supports the suggestion by Lyra et al. (2015) that *G. yoneshigueana* be synonymized with *G. domingensis* s.s. On account of this finding we make this formal proposal below.

Single-marker SDMs. Nearly all SDMs produced similar results with regard to the *G. domingensis* complex (Fig. 3, inset). Among the 17 accessions we included of the complex, seven, six, seven, ten, four, and six taxa were inferred for ABGD, SPN, GMYCs, GMYCm, PTP, bPTP, respectively. The log-likelihood ratio test results for GMYCs and GMYCm were significant ($P = 0.031$ and 0.0088, respectively).

Morphology and taxonomy. **Gracilaria baiana** G.M. Lyra, C.F.D. Gurgel, M.C. Oliveira & J.M.C. Nunes, **sp. nov.** (Fig. 4, a–h)

Holotype: Brazil, Bahia State, Praia da Penha, Vera Cruz city, 12°59′ 08.76″ S, 38°37′ 02.80″ W, *Coll. G.M. Lyra and J.M.C. Nunes*, 16 October 2010 (ALCB 103804), tetrasporophyte (Fig. 4a).

Isotype: *Coll. Lyra, G.M., and Nunes, J.M.C.* 16 October 2010 (ALCB 103799), female gametophyte.

Paratypes: same location. coll. Lyra, G.M. and Nunes, J.M.C., 01 September 2012 (ALCB103788), female gametophyte; coll. Lyra, G.M. and Nunes, J.M.C., 01 September 2012 (ALCB103789), male gametophyte; coll. Gurgel, C.F., 6 November 2002 (s/n), infertile.

Distribution: Brazil: Bahia, Vera Cruz, Praia da Penha.

Diagnosis: Thalli flattened throughout, soft, mostly dischotomously branched, with wart-like proliferations on the surface and henriquesiana-type spermatangia.

Etymology: named after the State of Bahia, Brazil.

Description: Thallus erect, flattened throughout, arising from small, rounded holdfasts; main axes strap-shaped (Fig. 4a), flaccid in texture, 10–15 (-18) cm tall, 2–3 mm wide, 740–885 μm thick, color pale yellow to pink, sometimes dark red in basal and lower parts of the thallus when growing in dense clumps; main axes dichotomously (rarely subdichotomously) branched up to 5 (-6) orders; branches gradually decreasing in width distally; lateral branches not constricted at base, mostly arising irregularly from the thallus margins. Apices variable, dichotomously divided, acute to round (Fig. 4b). Sharp transition in cell size between medullary and cortical regions; medulla composed of 5–8 layers of large, thin-walled, isodiametric cells, 102–306 μm wide; cortical region composed of 1–3 layers of radially elongated cells, 5–7 × 6–12 μm (Fig. 4c). Occasional trichomes emerging from enlarged cortical cells (Fig. 4h); trichomes are caducuous leaving behind a basal enlarged cell bearing a scar. Presence of cortical wart-like proliferations on both sides of the thallus, rounded in surface view, 70–108 μm wide, 40–65 μm tall (Fig. 4, g and h). Tetrasporangia decussate cruciate scattered in both sides of the blade, immersed in the cortical region; up to 30 μm in width, and 46 μm in length (Fig. 4c). Henriquesiana-type spermatangial conceptacles present on both sides of the blade (Fig. 4, d and e). Cystocarps wide at the base, scattered on lower and upper surfaces of

FIG. 1. Maximum likelihood (ML) phylogeny of *cox*1 (ntax = 33, missing data = 0.5%). Support values >75% are indicated. Values above branches are ML bootstrap values (left) and Bayesian posterior probabilities converted to percentages (right). An asterisk indicates that the node is supported at 100%. New sequences produced in this study in boldface; data otherwise from GenBank. Taxon names are followed by field ID numbers (new sequences) or GenBank accession numbers. The two subclades representing the *G. dominguensis* species complex are labeled I and II.
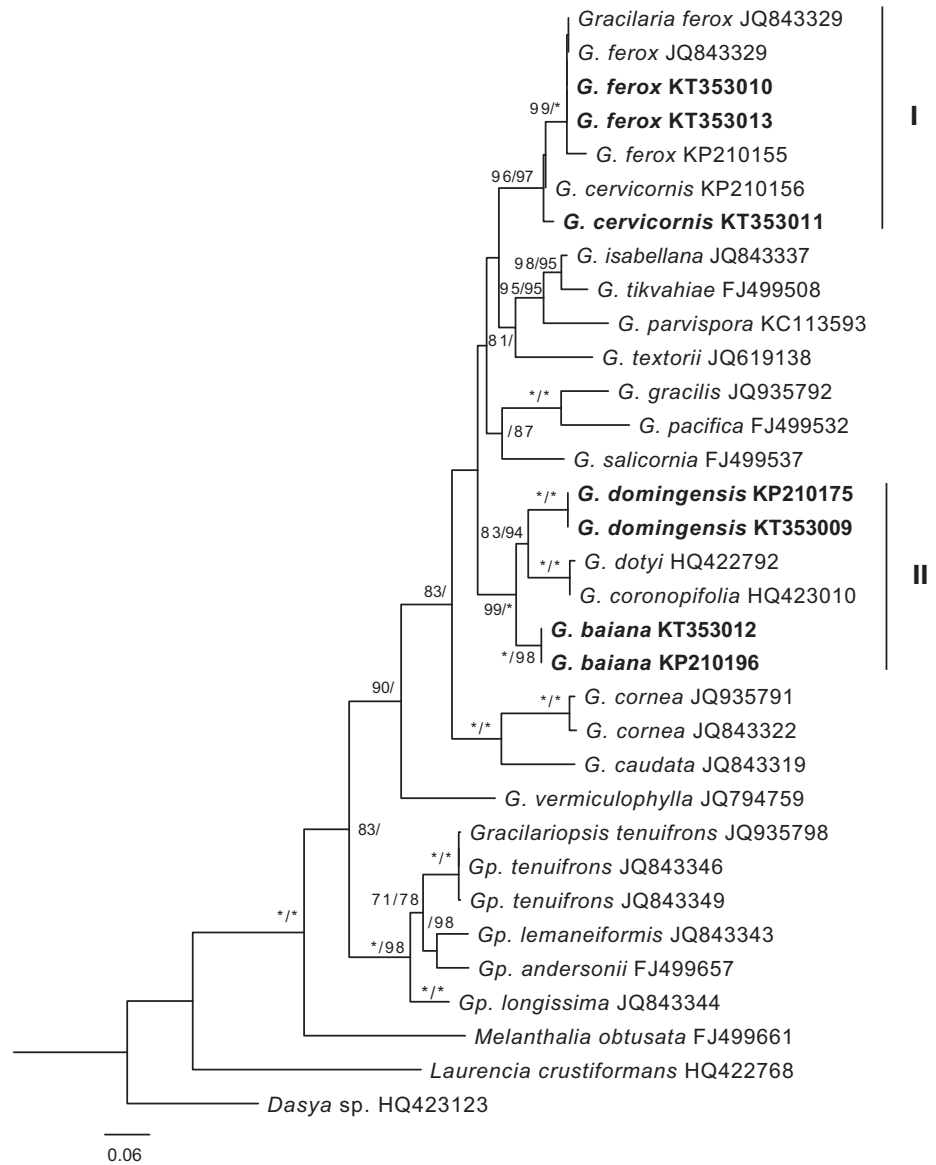
main axes, 1.0–1.5 mm wide, 0.8–1.0 mm tall; outer pericarp composed of 10–12 cell layers; carposporangia organized in irregularly packed branched files; gonimoblasts at maturity completely filling cystocarp cavity and composed of small, regular thin-walled cells; carpogonial fusion cell not pronounced; 3–4 layers of differenciated cells forming the cystocarp floor (inner pericarp); nutritive tubular cells connecting the gonimoblast to the outer pericarp (Fig. 4f).

Gracilaria cervicornis (Turner) J. Agardh 1852: 592 (Figs. 5, a–e; 6, a–e)

Basionym: *Fucus cervicornis* Turner

Type locality: Jamaica. LECTOTYPE: BM000936191

Homotypic Synonyms: *Fucus cervicornis* Turner 1808; *Sphaerococcus cervicornis* (Turner) C.Agardh 1817; *Rhodymenia cervicornis* (Turner) Montagne 1842

Heterotypic Synonyms: *Gracilaria acanthophora* (Kützing) Crouan (based on *Sphaerococcus acanthophorus* Kützing, which was previously synonymized under *Gracilaria acanthophora* by Schramm and Mazé, 1865, p. 218), *Gracilaria patens* var. *gracilis* P.L.Crouan & H.M.Crouan, type non vidi [(vide Dawes and Mathieson (2008, p. 342)].

Distribution: Argentina, Belize, Bermuda, Brazil, Cameroon, Canary Islands, Caribbean islands, Colombia, Equatorial Guinea, Ghana, Italy, Kenya, Mexico, Morocco, Panama, Seychelles, Spain, Tunisia, Southern United States, Venezuela. In Brazil, from Rio Grande do Norte to São Paulo. Specimens referred for Argentina, Seychelles and Spain possibly require confirmation as the species has equatorial, tropical, or subtropical distribution.

Description: Thalli erect, completely flattened, 6–35 cm tall, main axes sparsely and irregularly
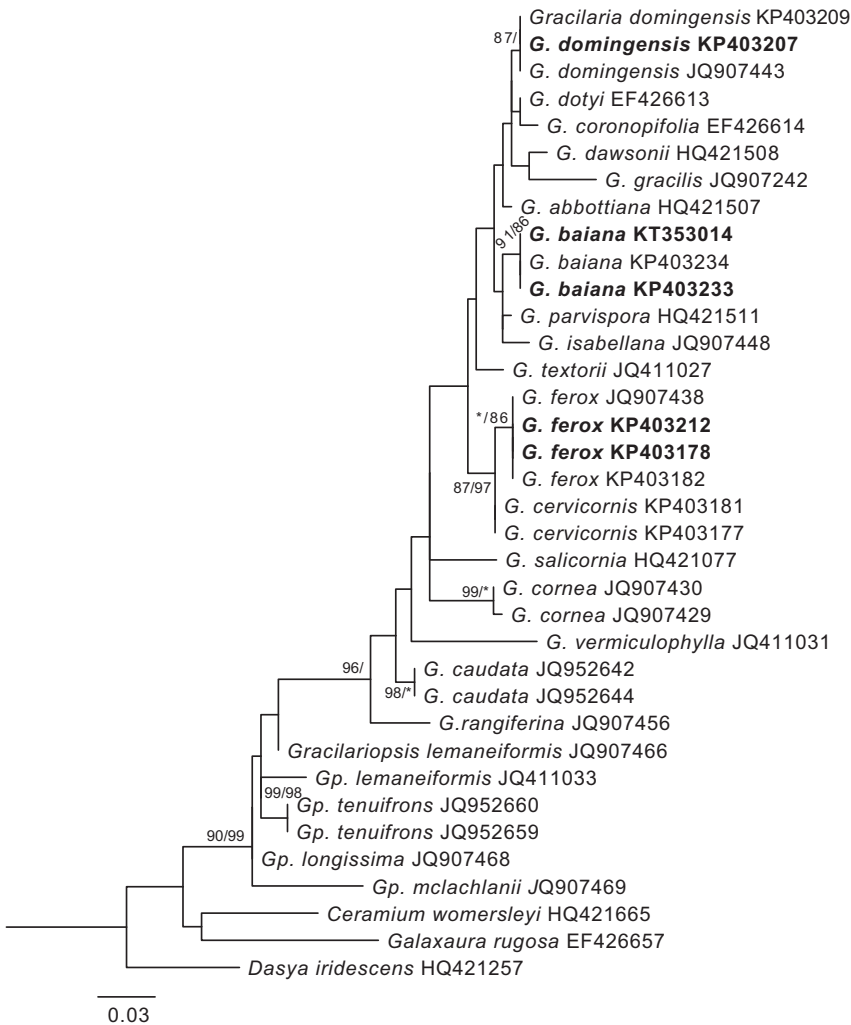
Fig. 2. Maximum likelihood (ML) phylogeny of UPA (ntax = 36, missing data = 0.5%). Support values >75% are indicated. Values above branches are ML bootstrap values (left) and Bayesian posterior probabilities converted to percentages (right). An asterisk indicates that the node is supported at 100%. New sequences produced in this study in boldface; data are otherwise from GenBank. Taxon names are followed by field ID numbers (new sequences) or GenBank accession numbers. The two subclades representing the *G. dominguensis* species complex are labeled I and II.

branched up to two orders. Dense spinescent branchlets inserted laterally and over the main axis and branches; branchlets denser in apical regions of the thallus, sometimes overcrowded. Apexes acute (Fig. 5, a–e). Medullary region with 4–6 layers of large hyaline cells; medullary cells with gradual transition toward cortical region; inner medullary cells up to 107 × 133 μm, subcortical elongated cells 55–62 μm in height, 75–94 μm wide; cortical cells 5–6 μm long by 8–9 μm wide (Fig. 6b). Decussate cruciate tetrasporangia immersed in both sides of the blade; tetrasporangia 6–8 μm wide, 15–20 μm long (Fig. 6a). Textorii-type spermatangial conceptacles distributed on both sides of the blade (Fig. 6, b and c). Cystocarps with slight constriction at the base forming pedunculated cystocarps; outer pericarp with 6–10 layers of cells; gonimoblasts and carposporangial chains irregularly organized; carpogonial fusion cell not pronounced; inferior nutritive tubular cells connecting the gonimoblast to the cystocarp floor (Fig. 6, d–e).

G. domingensis (Kützing) Sonder ex Dickie 1874: 149, plate 11. (Figs. 7, a–f; 8, a–d)

Basionym: *Sphaerococcus domingensis* Kützing

Type locality: Santo Domingo [Dominican Republic]. HOLOTYPE: MEL 44407

Homotypic Synonyms: *Sphaerococcus domingensis* Kützing 1869; *Polycavernosa domingensis* (Kützing) J.H. Price & D.M. John 1988

Heterotypic Synonyms: *Plocaria bipennata* P.L.Crouan & H.M.Crouan, *Plocaria polymorpha* P.L. Crouan & H.M. Crouan, and *Plocaria squarrosa* P.L. Crouan & H.M. Crouan, type non vidi [(vide Dawes and Mathieson (2008, p. 342)]; *Gracilaria yoneshigueana* Gurgel, Fredericq & J.N.Norris, new synonym (holotype: US Alg. Coll.-204329!).

Distribution: Barbados, Brazil, Colombia, Costa Rica, Cuba, Dominican Republic, Panama and Venezuela. In Brazil, from Maranhão to Santa Catarina.

Description: Thalli erect, flattened throughout, 10–15 (-26) cm tall, delicate to robust, fleshy, leathery to cartilaginous. Plants attached to the substratum by a roundish cushion-shaped holdfast. Thalli pale yellow to pink and red in color; smooth margins; irregularly, subdichotomously or pinnate

FIG. 3. Maximum likelihood (ML) phylogeny of *rbc*L (ntax = 95, missing data = 0%). Support values >75% are indicated. Values above branches are ML bootstrap values (left) and Bayesian posterior probabilities converted to percentages (right). An asterisk indicates that the node was supported at 100%. New sequences produced in this study in boldface; data are otherwise from GenBank. Taxon names are followed by field ID numbers (new sequences) or access numbers (sequences from Genbank). The two subclades representing the *G. dominguensis* species complex are labeled I and II. Inset displays SDM reconstructions. Gray filled bars represent taxon agreement with phylogenetic and morphological results. ABGD: automated barcode gap discovery, SPN: statistical parsimony network, GMYCs, generalized mixed Yule-coalescent model under the single threshold method, GMYCm, generalized Mixed Yule-coalescent model under the multiple threshold method, PTP: Poisson tree processes, and bPTP: Bayesian implementation of the Poisson Tree Process.
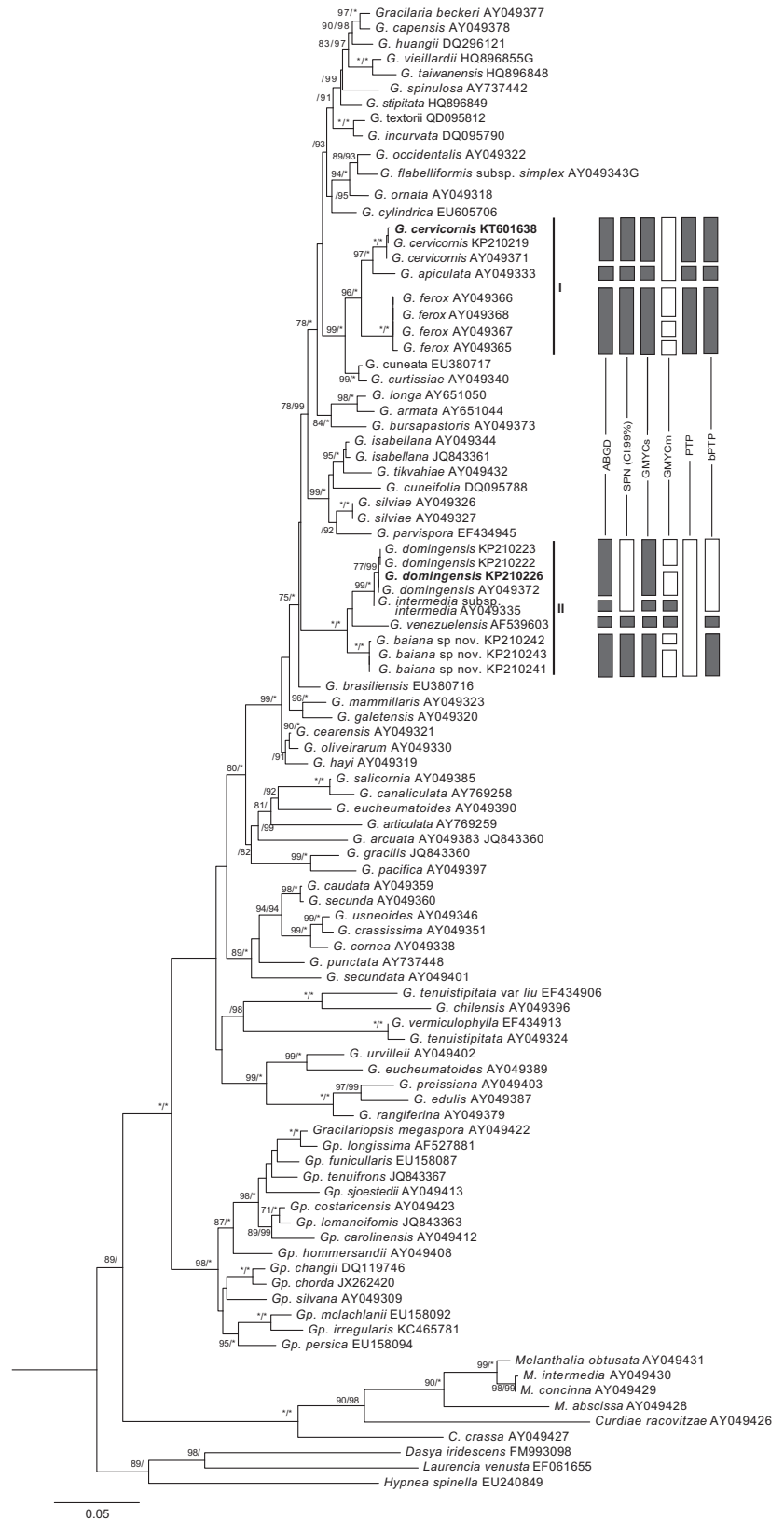
branched up to 3 (-4) orders (Fig. 7, a–f). Tetrasporophyte thalli with narrower main axes, 2–3 mm wide, with short lateral branches 2–10 mm wide (Fig. 7, c and e); male gametophytic main axes 3–5 mm wide, with branches and branchlets as long as the main axes, giving it a pinnate to bushy
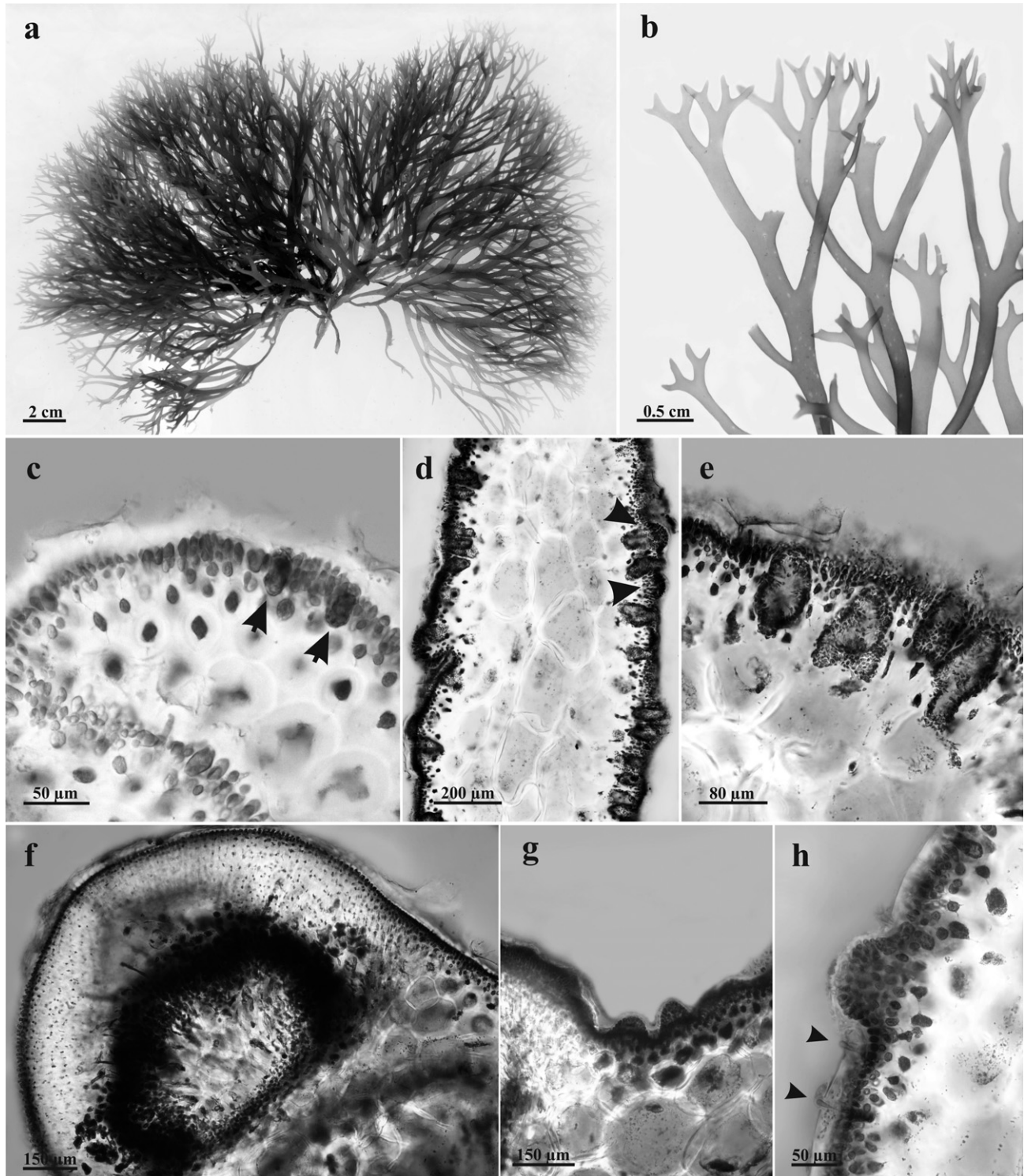
FIG. 4. Illustration of *Gracilaria baiana* sp. nov.: (a) habit of holotype, tetrasporophytic thallus; (b) detail of thallus showing apexes; (c) transverse section of a tetrasporophytic thallus, showing tetrasporangia (arrows); (d, e) transverse sections of male galetophytic thalli, showing spermatangia in deep conceptacles, henriquesiana type (arrows); (f) longitudinal section of a cystocarp; (g) transverse section of a female gametophytic thallus, showing wart-like proliferations in the cortical region; (h) transverse section of the cortical region of the thallus, showing a wart-like proliferation and two trichomes (arrows) arising from enlarged cortical cells (arrows).
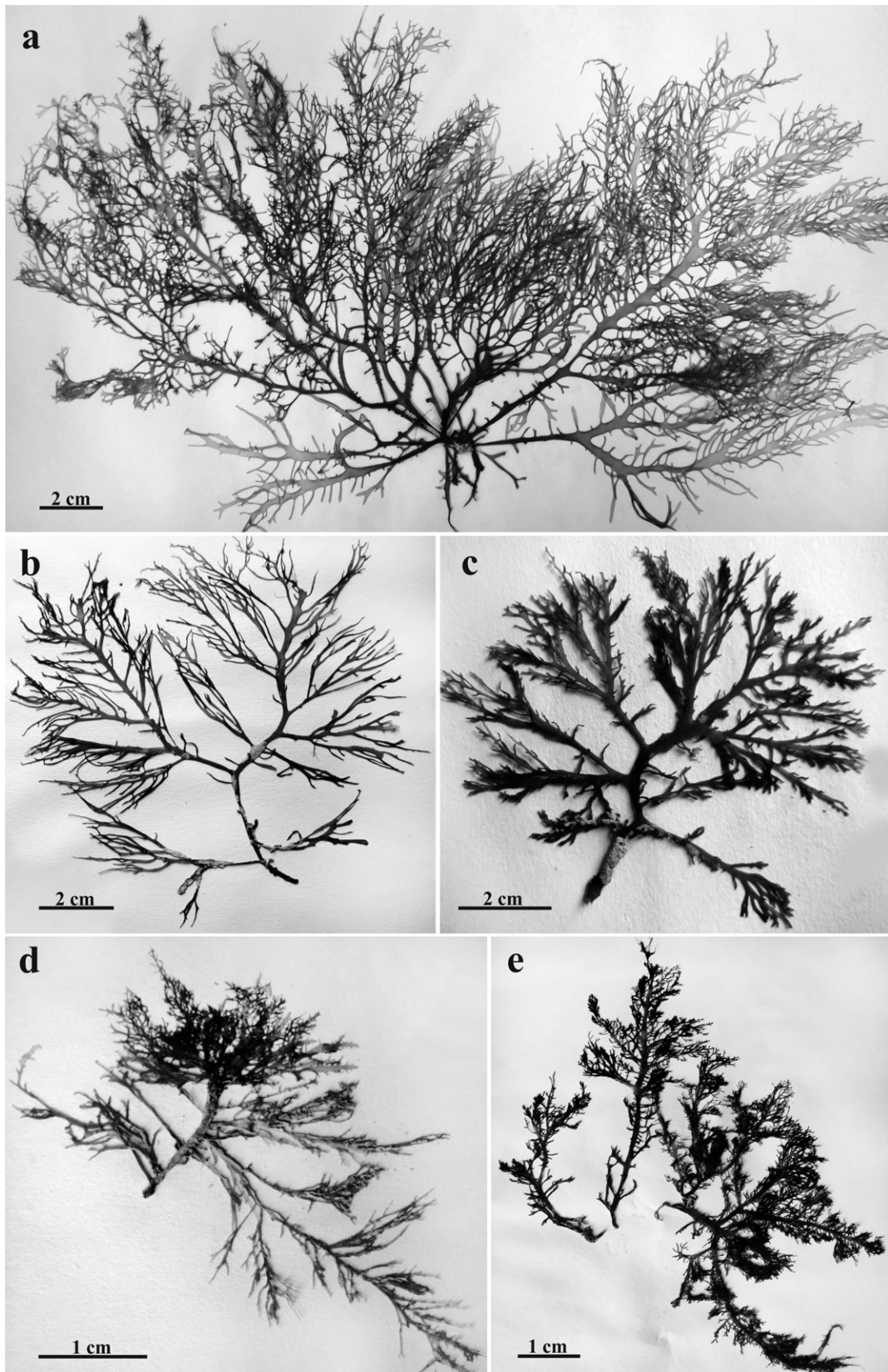
FIG. 5. *Gracilaria cervicornis* habit: (a, c, e) tetrasporophytes; (b) female gametophyte; (d) male gametophyte.
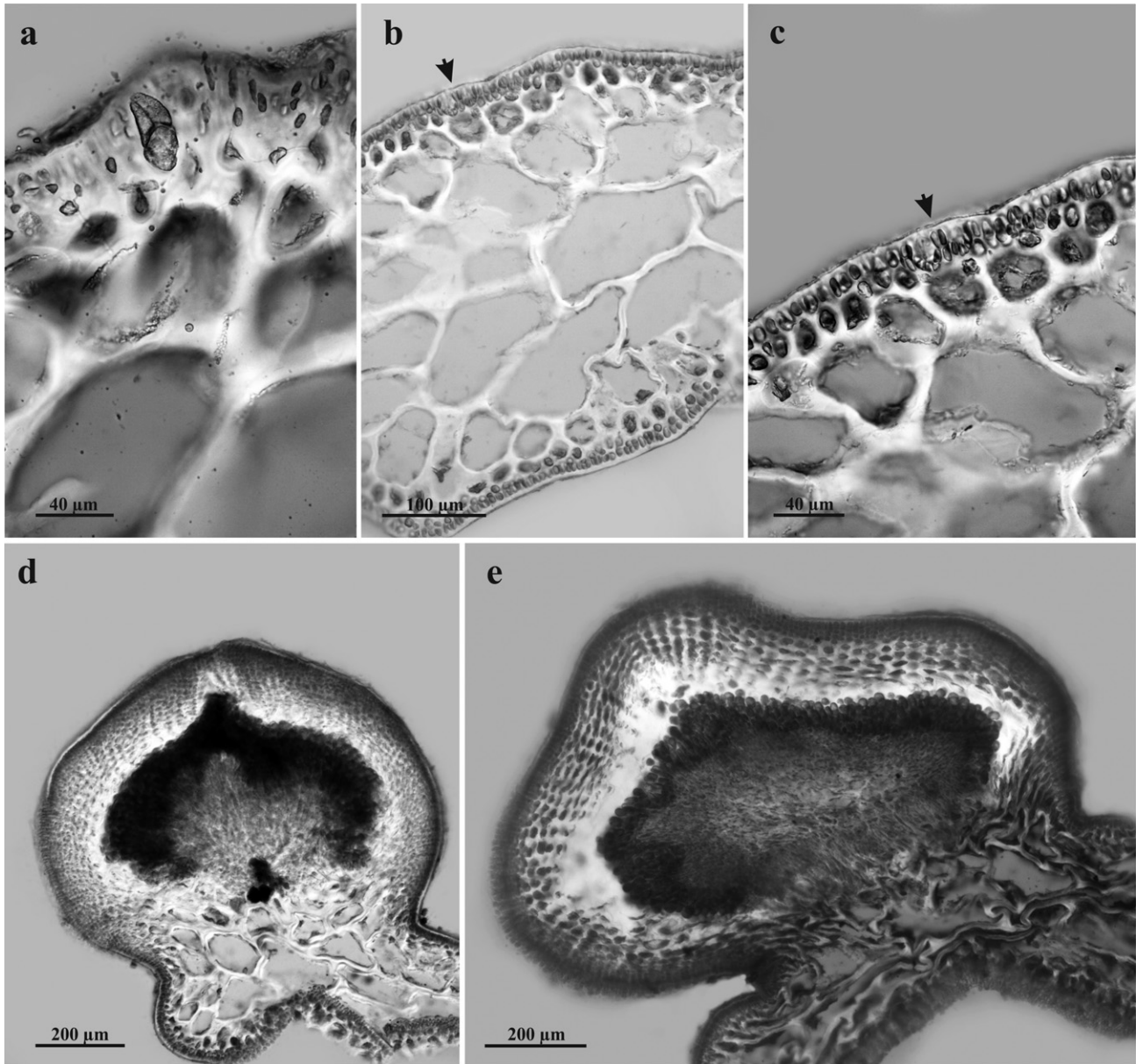
Fig. 6. *Gracilaria cervicornis* anatomical features: (a) transverse section of a tetrasporophytic thallus, showing tetrasporangia immersed in the cortical region; (b) transverse section of male gametophytic thallus, showing spermatangia in shallow conceptacles, textorii type (arrows); (c) amplification of the structure shown in b. (d, e) longitudinal sections of cystocarps.

appearance, with few long branchlets with acute axes sometimes dichotomously divided (Fig. 7, a, b and f); female gametophytic thalli larger, 5–15 mm wide, main axis bearing profuse number of branchelets of various sizes, inserted laterally on both opposite sides of the main axes, occasionally on the face (Fig. 7d). Sharp transition between medullary and cortical regions; medullary cells elliptical, 12–25 μm by 87–145 μm; cortical region composed of 2–3 cell layers, cortical cels 5–8 μm wide, 7–10 μm long (Fig. 8a). Decussate cruciate tetrasporangia, radially elongated, up to 20 μm wide, 35 μm long,

immersed in both sides of the thallus (Fig. 8a). Spermatangia distributed in deep, henriquesiana type, conceptacles on both sides of the thallus (Fig. 8, b and c). Cystocarps prominent, wide based, with slight basal constriction, pericarp composed of 15–21 cell layers; gonimoblasts and carposporangial chains irregularly organized; carpogonial fusion cell not pronounced; 3–5 layers of differentiated cells forming the cystocarp floor (inner pericarp); superior and inferior tubular cells connecting the gonimoblast to the outer pericarp and the cystocarp floor (Fig. 8d).

Gracilaria ferox J. Agardh 1852: 592 (Fig. 9, a–e)

Type locality: Martinique. LECTOTYPE: NY01089159

Distribution: Barbados, Bermuda, Brazil, Caicos Islands, Canary Islands, Jamaica, Colombia, Costa Rica, Cuba, Hispaniola, Lesser Antilles, Martinique, Mexico, Panama, Puerto Rico, Trinidad, southern United States, Venezuela, Virgin Islands. In Brazil: Bahia, Pernambuco.

Description: Thallus erect, flattened in most parts, up to 38 cm tall, attached to the substratum by a cushion-like holdfast. Axes intensely and irregularly ramified, with compressed or subterete branches at various levels, especially in the apical region, forming apical tufts (Fig. 9a); branch apices cervicornate ultimate divisions (Fig. 9b). Medullary region with 2–5 layers of hyaline cells; medullary cells with gradual transition toward cortical region; inner medullary cells 30 μm by 65 μm, subcortical medullary cells 12–15 μm in diameter (Fig. 9c). Tetrasporangia decussate cruciate immersed on both sides of the blade (Fig. 9c). Spermatangia of the textorii type on both sides of the blade (Fig. 9d). Cystocarps prominent, pericarp with 8–12 cell layers; gonimoblasts and carposporangial chains irregularly organized; nutritive tubular cells absent (Fig. 9e).

Dichotomous key for the identification of species in the G. domingensis *complex.*

1a	Thallus not entirely flattened, compressed to subcylindrical portions	2
2a	Branches in one plane with numerous branchlets arranged marginally	*G. venezuelensis* (Fig. 2; Gurgel et al. 2004a)
2b	Branches in more than one plane with numerous branchlets arranged radially	3
3a	Thallus delicate, slender with 2–5 layers of small medullary cells 35–65 μm in length	*G. ferox* (Fig. 9)
3b	Thallus robust, with 6–12 layers of large medullary cells 125.7–174.7 μm in length	*G. apiculata* subsp. *apiculata* (Figs. 3–6, Gurgel et al. 2004b)
1b	Thallus entirely flattened, without compressed to subcylindrical portions	4
4a	Thallus markedly dichotosmously branched, with warts covering its surface	*G. baiana* sp. nov. (Fig. 4)
4b	Thallus irregularly branched, without warts covering its surface	5
5a	Thallus 1–3 mm wide, spermatangia in shallow, textorii type conceptacles	*G. cervicornis* (Figs. 5 and 6)
5b	Thallus 2 mm–4 cm wide, spermatangia in deep, verrucosa or henriquesiana type conceptacles	6
6a	Thallus 3–4 cm wide, terminal branchlets of long branches with expanded rounded or obtuse	*G. intermedia* subsp. *intermedia* (Fig. 3, a and b,

(continued)

apices, medullary cells 224.6–274.5 μm long by 109.8–144.7 μm wide Gurgel et al. 2004a)

6b	Thallus 2–15 mm wide, terminal branchlets of long branches with acute, frequently lacerate apices, medullary cells 12–25 μm long by 87–145 μm wide	*G. domingensis* (Figs. 7 and 8)

DISCUSSION

Our three-pronged approach to delimiting species in the *G. domingensis* complex identifies seven well-defined species, belonging to two distantly related clades (Figs. 1-3): *G. cervicornis*, a ressurected *G. ferox*, and *G. apiculata* subsp. *apiculata* (clade I); a new species *G. baiana* sp. nov., *G. intermedia* subsp. *intermedia*, *G. venezuelensis*, and *G. domingensis* s.s. (clade II). This integrated approach has been favored in the scientific community because it makes use of the broadest range of independent data types, greatly improving taxonomic robustness (e.g., Gurgel et al. 2008, Goldstein and De Salle 2011, Puillandre et al. 2012b). We discuss below the three lines of evidence we employed for species delimitation, focusing first on the results of our SDMs and then moving to a discussion of the phylogeny and morphology of the relevant species.

Single-marker methods and species delineation. Nearly all six SDMs support our circumscription of the *G. domingensis* complex (Fig. 3, inset). The only variation we detected in this delimitation was to combine species in four cases (GMYCm: *G. cervicornis* and *G. apiculata* subsp. *apiculata*; SPN: *G. domingensis* and *G. intermedia* subsp. *intermedia*; PTP: *G. domingensis*, *G. venezuelensis*, *G. intermedia* subsp. *intermedia*, and *G. baiana* sp. nov.; bPTP: *G. domingensis*, *G. intermedia*) or to split a species in one case (GMYCm: *G. ferox*, *G. domingensis*, and *G. baiana* sp. nov.). Such variation in SDMs is not entirely surprising, however, and is relatively common for these sorts of analyses (reviewed in Talavera et al. 2013). Factors that may influence these differences include the geographic distribution of samples (Bergsten et al. 2012, Talavera et al. 2013), and the estimation of population genetic parameters, including effective population size and speciation rate (Esselstyn et al. 2012). Furthermore, species estimated error rates have been shown to vary between individual lineages (Hendrich et al. 2010) with overestimation and underestimation of the true number of taxa reaching values as high as 21% depending on the method implemented (e.g., Tänzler et al. 2012). Given the general consensus among models, combined with our inferences of phylogeny and morphology discussed below, we favor the four species delimitation proposed above.

Morphological delimitation of species. The identification of discrete morphological entities in the
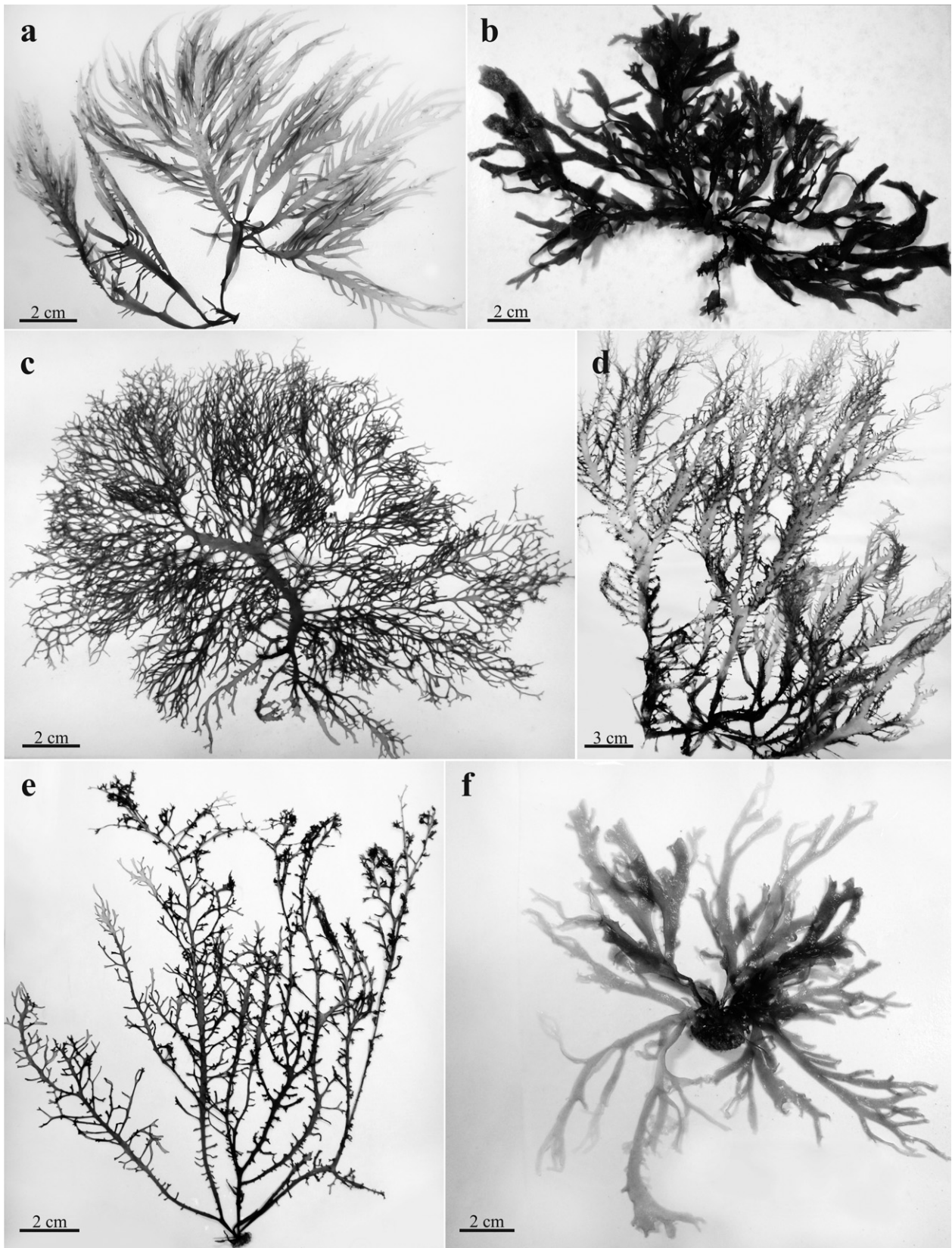
FIG. 7. *Gracilaria domingensis* sensu stricto different morphotypes: (a, b, f) male gametophytes; (c, e) tetrasporophytes; (d) female gametophyte.
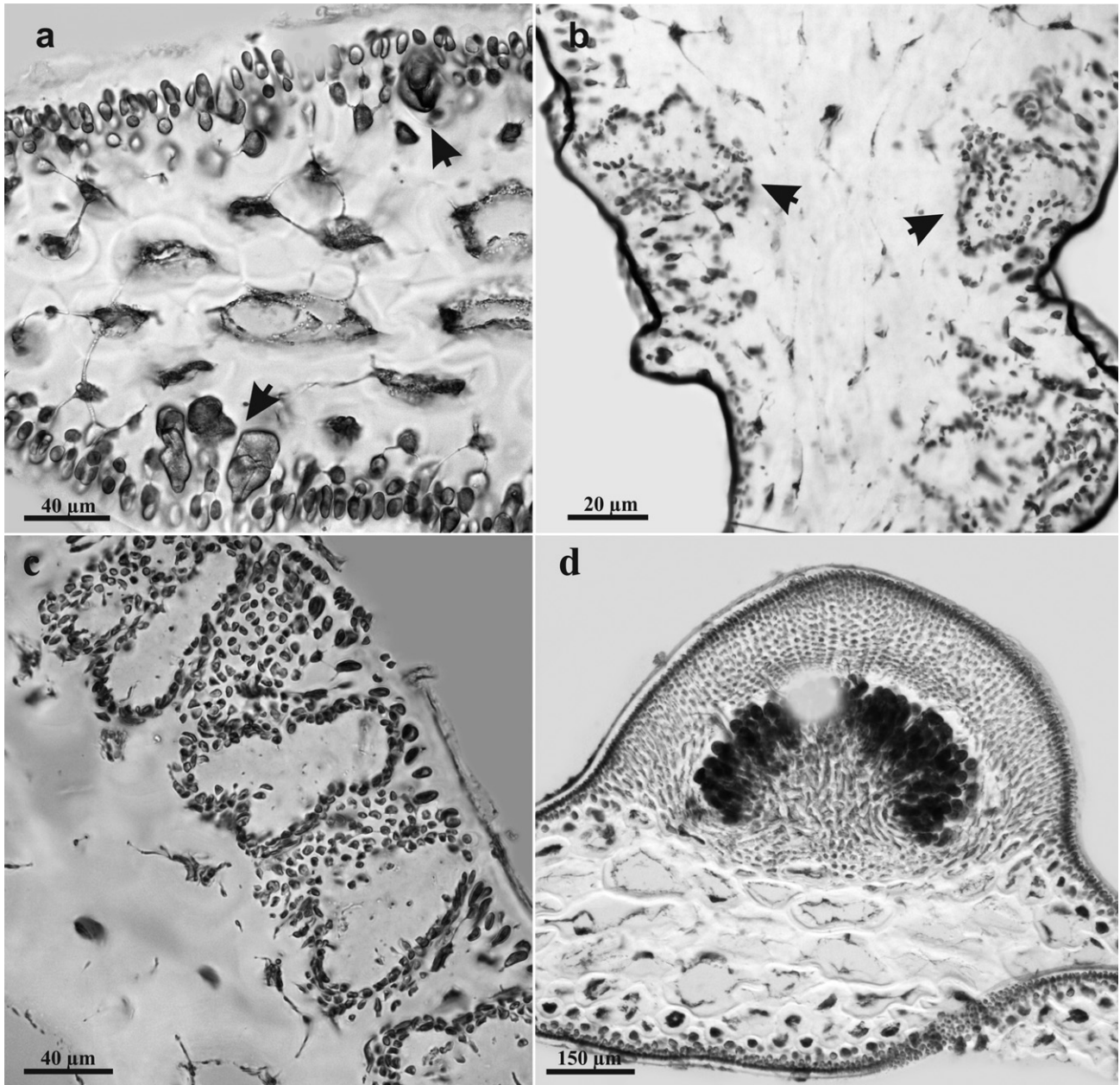
Fig. 8. *Gracilaria domingensis* sensu stricto anatomical features: (a) transverse section of a tetrasporophytic thallus, showing tetrasporangia on both sides of the blade (arrows); (b, c) transverse section of male gametophytic thallus, showing spermatangia in deep conceptacles, henriquesiana type (arrows); (d) longitudinal section of a cystocarp.

G. domingensis species complex has made this a challenging group. This is due in part to the extent of homoplasy of especially male reproductive structures in the family. For example, the heriquesiana-type spermatangial conceptacle, once thought to be diagnositic for genera of Gracilariaceae, was recently demonstrated (Lyra et al. 2015) to have arisen independently in *G. domingensis* and *G. rangiferina*. Furthermore, tremendous habit variation exists within this complex, including at least five distinct morphotypes. These morphotypes can (with limits) be associated with unique life cycles and reproductive stages (Fig. 7, a–f), but are not readily distinguishable from other species in the complex.

The morphological similarity among the four cryptic species we describe here helps to explain the lack of taxonomic clarity in this complex. This has been especially aggravating for field workers with untrained eyes because *G. cervicornis*, *G. ferox*, *G. domingensis* s.s., and *G. baiana* can be found growing together in the same site, apparently sharing the same microenvironment (ecological niche). This is even more perplexing given the phylogenetic distance between some of these taxa. We identify here
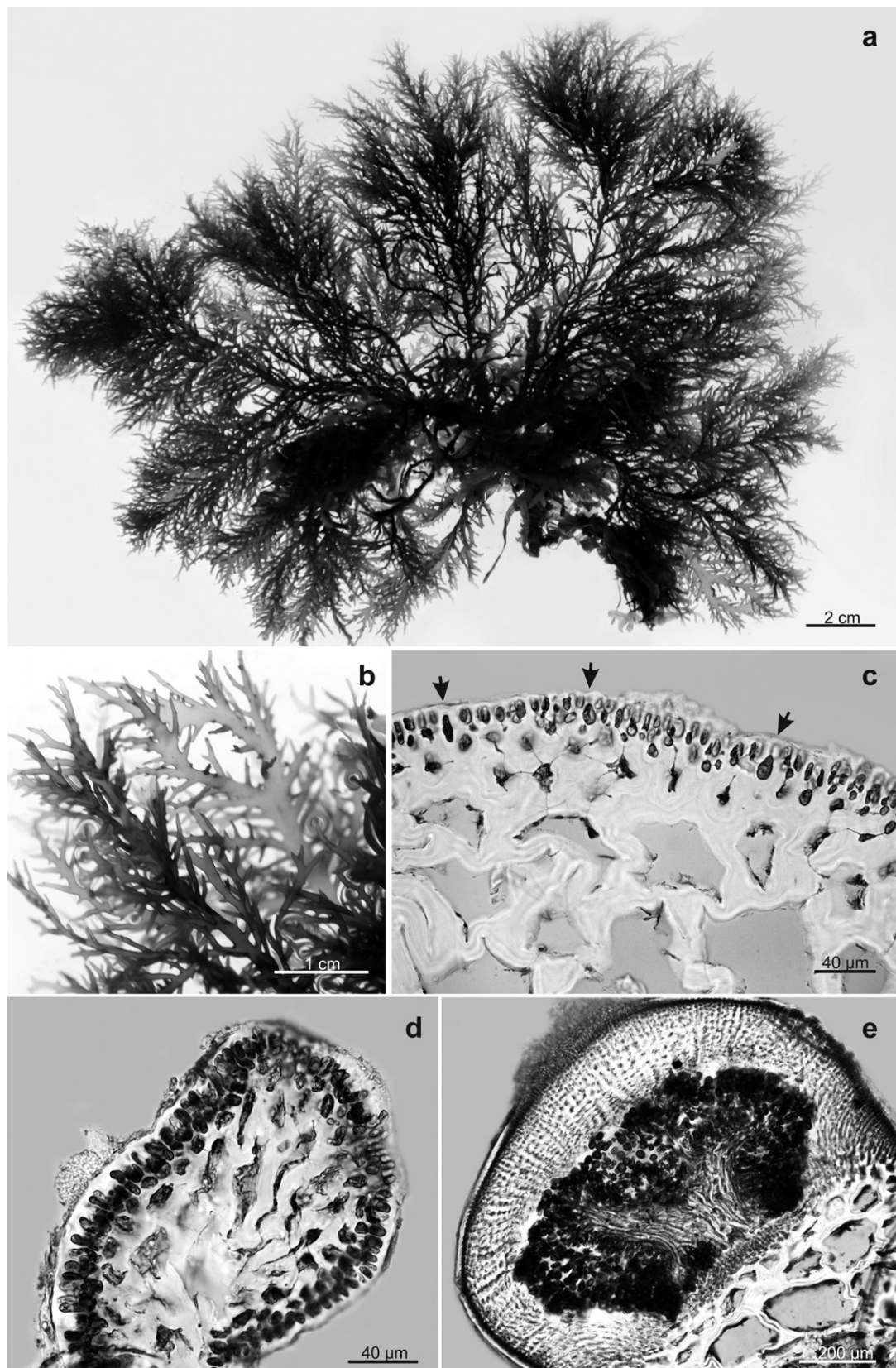
FIG. 9. Illustration of *Gracilaria ferox*: (a) habit; (b) details of the apical region, showing braching in all planes; (c) transverse section of a tetrasporophytic thallus, showing tetrasporangia (arrows); (d) transverse section of male gametophytic thallus, showing spermatangia in shallow conceptacles, textorii type; (e) longitudinal section of a cystocarp.

that although all individuals of a species are monophyletic, members of this complex are not monophyletic and can in some cases be relatively distantly related (e.g., *G. cervicornis* and *G. domingensis*; Fig. 3). Here, we describe the morphological and phylogenetic grounds for distinguishing these species.

Clade I: *G. cervicornis*, *G. ferox*, and *G. apiculata* subsp. *apiculata*

Gracilaria cervicornis and *G. ferox* were previously synonymized by Oliveira et al. (1983). However, our phylogeny and SDMs are all consistent with the separation of these two species (Fig. 3). Morphology further supports this concept. *Gracilaria cervicornis* thalli tend to be completely flattened, more delicate, with branches and branchlets arising mostly from one plane, usually along the margins of the main axes (Fig. 5). In contrast, *G. ferox* exhibits thalli with terete to subcylindrical distal regions, branches and branchlets in multiple planes, especially close to the apices, forming three-dimensional tufts (Fig. 9, a and b). Our new morphological characterization of *G. ferox* has been misapplied to *G. cervicornis* across the western Atlantic. Hence, we call attention to phycologists that, going forward, highly branched tuft-forming specimens (= bushy) belonging to the *G. cevicornis*–*G. ferox* lineage be attributed to *G. ferox*. Lastly, these two species share spermatangial conceptacles of the textorii type (Figs. 6, b and c; 9d).

A third species in this clade, *G. apiculata* subsp. *apiculata*, is identified as the well-supported sister to *G. cervicornis*. The morphology of *G. apiculata* subsp. *apiculata* is thought to be distinct based on morphology (Gurgel et al. 2004b), but the paucity of specimens for this species makes this difficult to verify. In particular, there is no available data regarding its spermatangial conceptacle type.

Clade II: *G. domingensis* s.s, *G. baiana* sp. nov., *G. venezuelensis*, and *G. intermedia* subsp. *intermedia*

Among the species we circumscribe, *G. baiana* sp. nov., is new to science. Specimens of *G. baiana* sp. nov. are phylogentically distinct from other *Gracilaria* species (Fig. 3), and at least adult specimens of this species are morphologically distinct. Among the five specimens included in our study, it was possible to verify mature stages of all reproductive structures (i.e., male, female, and tetrasporic). *G. baiana* specimens were found only in the type locality, growing intertidally, and forming dense tufts inside coastal reef lagoons. When compared with its close relative and morphologically similar, *G. domingensis* s.s, thalli of *G. baiana* are thicker, more flaccid, markedly dichotomously branched, and exhibit characteristic cortical proliferations (warts) scattered across the thallus (visible in the stereomicroscope; Figs. 4 and 7). Besides habit similarities, both *G. baiana* and *G. domingensis* s.s. have the same type of spermatangial conceptacle, the heriquesiana type (Figs. 4, d–e; 8c). For this reason, *G. baiana* may be confused with *G. domingensis*.

However, the branching pattern of the thalli and the presence of warts on the thallus surface help to differentiate *G. baiana*.

Our phylogeny (Fig. 3) identifies two additional members of this clade: *G. intermedia* subsp. *intermedia* and *G. venezuelensis*, which are successive sister species to *G. domingensis* s.s. *G. intermedia* subsp. *intermedia* possesses the verrucosa type of spermatangial conceptacle (Gurgel et al. 2004a), which likely represents a different stage in the developmental series of the heriquesiana type present in *G. domingensis* s.s. (Abbott et al. 1991, Lyra et al. 2015). *Gracilaria venezuelensis* has compressed portions of the main axis, and subcylindrical branchlets, which makes it quite distinct morphologically from its closest relatives *G. baiana*, *G. intermedia*, and *G. domingensis* (Gurgel et al. 2004a).

Lastly, our newly generated *rbc*L sequences from large *G. domingensis* s.s. specimens (>30 cm tall plants) were identical to those deposited in GenBank as *G. yoneshigueana* (AY049372; Gurgel et al. 2004a). *Gracilaria. yoneshigueana* was described from minute plants (<2 cm), which were nevertheless fertile (tetrasporic). Thus, our results indicate that *G. yoneshigueana* corresponds to juveniles of *G. domingensis* s.s. and that *G. domingensis* tetrasporophytes can become fertile after growing only a few centimeters tall. We therefore synonymized *G. yoneshigueana* with *G. domingensis* s.s as previously suggested by Lyra et al. (2015). This finding underscores the fact that juvenile material of species in the *G. domingensis* complex may be nearly impossible to identify without DNA barcoding.

CONCLUSION

Our study greatly clarifies the *G. domingensis* species complex. Here, we recognize seven species in two different clades, including one species new to science, *G. baiana* sp. nov. We recircumscribed *G. domingensis* s.s. and *G. cervicornis*, which are abundant species in the western Atlantic Ocean, reestablished *G. ferox*, and synonymized *G. yoneshigueana* with *G. domingensis* s.s. Using a combination of classical taxonomy and multimarker molecular-based analyses, it was possible to advance our understanding of the systematics of this common, but difficult, group of marine benthic flora. Going forward, larger sampling including specimens from different localities would be important to provide a better assessment of intraspecific variation across all taxa. However, at least for *G. baiana*, this is not yet possible because this taxon has been found only in its type locality.

Abbott, I. A., Zhang, J. & Xia, B. 1991. *Gracilaria mixta* sp. nov. and other western Pacific species of the genus (Rhodophyta: Gracilariaceae). *Pacif. Sci.* 45:12–27.

Almeida, C. L. F., Falcão, H. S., Lima, G. R. M., Montenegro, C. A., Lira, N. S., Athayde-Filho, P. F., Rodrigues, L. C., Souza, M. F. V., Barbosa-Filho, J. M. & Batista, L. M. 2011. Bioactivities from marine algae of the Genus *Gracilaria. Int. J. Mol. Sci.* 12:4550–73.

Bergsten, J., Bilton, D. T., Fujisawa, T., Elliott, M., Monaghan, M. T., Balke, M., Hendrich, L. et al. 2012. The effect of geographical scale of sampling on DNA barcoding. *Syst. Biol.* 61:851–69.

Clement, M., Posada, D. C. K. A. & Crandall, K. A. 2000. TCS: a computer program to estimate gene genealogies. *Mol. Ecol.* 9:1657–9.

Cohen, S., Faugeron, S., Martínez, E. A., Correa, J. A., Viard, F., Destombe, C. & Valero, M. 2004. Molecular identification of two sibling species under the name *Gracilaria chilensis* (Rhodophyta, Gracilariales). *J. Phycol.* 40:742–7.

Costa, E. S., Plastino, E. M., Petti, R., Oliveira, E. C. & Oliveira, M. C. 2012. The Gracilariaceae Germplasm Bank of the University of São Paulo, Brazil - a DNA barcoding approach. *J. Appl. Phycol.* 24:1643–53.

Dawes, C. J. & Mathieson, A. C. 2008. *The seaweeds of Florida.* University Press of Florida, USA, 591 pp.

Drummond, A. J., Ashton, B., Buxton, S., Cheung, M., Cooper, A., Duran, C., Field, M. et al. 2011. Geneious v6.0.6. Available at http://www.geneious.com (last accessed 30 January 2016).

Esselstyn, J. A., Evans, B. J., Sedlock, J. L., Khan, F. A. A. & Heaney, L. R. 2012. Single-locus species delimitation: a test of the mixed Yule–coalescent model, with an empirical application to Philippine round-leaf bats. *Proc. R. Soc. Lond. B* 279:3678–3686.

Faugeron, S., Valero, M., Destombe, C., Martinez, E. A. & Correa, J. A. 2001. Hierarchical spartial struture and discriminant analysis of genetic diversity in the red alga *Mazzaella laminarioides* (Gigartinales, Rhodoplyta). *J. Phycol.* 37:705–17.

Freshwater, D. W. & Rueness, J. 1994. Phylogenetic relationships of some European *Gelidium* (Gelidiales, Rhodophyta) species based on *rbc*L nucleotide sequence analysis. *Phycologia* 33:187–94.

Goldstein, P. Z. & De Salle, R. 2011. Integrating DNA barcode data and taxonomic practice: determination, discovery and description. *BioEssays* 33:135–47.

Guiry, M. D. & Guiry, G. M. 2016. AlgaeBase. Worldwide electronic publication, National University of Ireland, Galway. Available at http://www.algaebase.org (last accessed 28 April 2016).

Gurgel, C. F. D. & Fredericq, S. 2004. Systematics of the Gracilariaceae (Gracilariales, Rhodophyta): a critical assessment based on *rbcl* sequence analysis. *J. Phycol.* 40:138–59.

Gurgel, C. F. D., Fredericq, S. & Norris, J. N. 2004a. Molecular systematics and taxonomy of flattened species of *Gracilaria* Greville (Gracilariaceae, Gracilariales, Rhodophyta) from the Western Atlantic. *In* Abbott, I. A. & McDermid, K. [Eds.] *Taxonomy of Economic Seaweeds IX* (with reference to the Pacific and other locations). California Sea Grant College, University of California, La Jolla, California, pp. 159–99.

Gurgel, C. F. D., Fredericq, S. & Norris, J. N. 2004b. *Gracilaria apiculata* and *G. flabelliformis* (Gracilariales, Rhodophyta): restoring old names for common tropical western Atlantic species, including the recognition of three new subspecies, and a replacement name for "*G. lacinulata*". *Cryptog. Algol.* 25:367–96.

Gurgel, C. F. D., Fredericq, S., Norris, J. N. & Yoneshigue-Valentin, Y. 2008. Two news flat species of *Gracilaria* (Gracilariales, Rhodophyta) from Brazil: *G. abyssalis* sp. nov. and *G. brasiliensis* sp. nov. *Phycologia* 47:249–64.

Hendrich, L., Pons, J., Ribera, I. & Balke, M. 2010. Mitochondrial cox1 sequence data reliably uncover patterns of insect diversity but suffer from high lineage-idiosyncratic error rates. *PLoS ONE* 5:e14448.

Hillis, D. M. & Bull, J. J. 1993. An empirical test of bootstrapping as a method for assessing confidence in phylogenetic analysis. *Syst. Biol.* 42:182–92.

Holmgren, P. K., Holmgren, N. H. & Barnett, L. C. [Eds.] 1990. *Index Herbariorum. Part I: The Herbaria of the World,* 8th edn. New York, New York Botanical Garden, 693 pp.

Jukes, T.H. & Cantor, C.R. 1969. Evolution of protein molecules. In Munro, H. N. [Ed.] *Mammalian Protein Metabolism.* Academic Press, New York, pp. 21–132.

Lyra, G. M., Costa, E. S., Jesus, P. B., Matos, J. C. G., Caires, T. A., Oliveira, M. C., Oliveira, E. C., Xi, Z., Nunes, J. M. C. & Davis, C. C. 2015. Phylogeny of Gracilariaceae (Rhodophyta): evidence from plastid and mitochondrial nucleotide sequences. *J. Phycol.* 51:356–66.

Monaghan, M. T., Wild, R., Elliot, M., Fujisawa, T., Balke, M., Inward, D. J. G., Lees, D. C., Ranaivosolo, R., Eggleton, P., Barraclough, T. G. & Vogler, A. P. 2009. Accelerated species inventory on Madagascar using coalescent-based models of species delineation. *Syst. Biol.* 58:298–311.

Oliveira, E. C., Bird, C. J. & Mclachlan, J. 1983. The genus *Gracilaria* (Rhodophyta, Gigartinales) in the westerns Atlantic. *Gracilaria domingensis, G. cervicornis,* and *G. ferox. Can. J. Bot.* 61:2999–3008.

Pagel, M. & Meade, A. 2004. A phylogenetic mixture model for detecting pattern-heterogeneity in gene sequence or character-state data. *Syst. Biol.* 53:571–81.

Pons, J., Barraclough, T., Gomez-Zurita, J., Cardoso, A., Duran, D., Hazell, S., Kamoun, S., Sumlin, W. & Vogler, A. 2006. Sequence-based species delimitation for the DNA taxonomy of undescribed insects. *Syst. Biol.* 55:595–610.

Puillandre, N., Lambert, A., Brouillet, S. & Achaz, G. 2012a. ABGD, Automatic Barcode Gap Discovery for primary species delimitation. *Mol. Ecol.* 21:1864–77.

Puillandre, N., Modica, M. V., Zhang, Y., Sirovich, L., Boisselier, M. C., Cruand, C., Holford, M. & Samadi, S. 2012b. Large scale species delimitation method for hyperdiverse groups. *Mol. Ecol.* 21:2671–91.

Saunders, G. W. 2005. Applying DNA barcoding to red macroalgae: a preliminary appraisal holds promise for future application. *Philos. Trans. R. Soc.* 360:1879–88.

Schramm, A. & Mazé, H. 1865. *Essai de classification des algues de la Guadeloupe.* [1st Edition]. Imprimerie du Gouvernement, Basse-Terre, Guadeloupe, ii+52 pp.

Sherwood, A. R. & Presting, G. G. 2007. Universal primers amplify a 23S rDNA plastid marker in eukaryotic algae and cyanobacteria. *J. Phycol.* 43:605–8.

Stamatakis, A. 2006. RAxML-VI-HPC: maximum likelihood-based phylogenetic analyses with thousands of taxa and mixed models. *Bioinformatics* 22:2688–90.

Stamatakis, A., Hoover, P. & Rougemont, J. 2008. A rapid bootstrap algorithm for the RAxML web servers. *Syst. Biol.* 57:758–71.

Talavera, G., Dincă, V. & Vila, R. 2013. Factors affecting species delimitations with the GMYC model: insights from a butterfly survey. *Methods Ecol. Evol.* 4:1101–10.

Tänzler, R., Sagata, K., Surbakti, S., Balke, M. & Riedel, A. 2012. DNA barcoding for community ecology-how to tackle a hyperdiverse, mostly undescribed Melanesian fauna. *PLoS ONE* 7:e28832.

Thiers, B. [continuously updated]. 2014. Index Herbariorum: A global directory of public herbaria and associated staff. New York Botanical Garden's Virtual Herbarium. Available at http://sweetgum.nybg.org/ih/ (last accessed 30 January 2016).

Tsuda, R. T. & Abbott, I. A. 1985. Collecting, handling, preservation, and logistics. *In* Littler, M. M. & Littler, D. S. [Eds.]

Handbook of Phycological Methods, Vol. IV. Ecological Field Methods: Macroalgae. Cambridge Univ. Press, Cambridge/New-York, pp. 67–86.

Venditti, C., Meade, A. & Pagel, M. 2008. Phylogenetic mixture models can reduce node-density artifacts. *Syst. Biol.* 57:286–93.

Wakeley, J. 2009. *Coalescent Theory: An Introduction.* Roberts & Company Publishers, Greenwood Village, Colorado.

Xi, Z., Ruhfel, B. R., Schaefer, H., Amorim, A. M., Sugumaran, M., Wurdack, K. J., Endress, P. K., Matthews, M. L., Stevens, P. F., Mathews, S. & Davis, C. C. 2012. Phylogenomics and a posteriori data partitioning resolve the Cretaceous angiosperm radiation Malpighiales. *Proc. Natl. Acad. Sci. USA* 109:17519–24.

Yamamoto, H. 1984. An evaluation of some vegetative features and some interesting problems in Japanese populations of *Gracilaria. Hydrobiologia* 116/117:51–4.

Yule, G. U. 1925. A mathematical theory of evolution, based on the conclusions of Dr. J. C. Willis. *F.R.S. Philos. Trans. R. Soc. Lond. B (containing papers of a biological character)* 213:21–87.

Zhang, J., Kapli, P., Pavlidis, P. & Stamatakis, A. 2013. A general species delimitation method with applications to phylogenetic placements. *Bioinformatics* 29:2869–2876.